Physics – Uspekhi **55** (11) 1061 – 1079 (2012)

REVIEWS OF TOPICAL PROBLEMS PACS numbers: **62.10.+s**, **62.50.–p**, **63.50.–x**, 64.60.F–, 64.60.fd, 65.20.De, 66.20.Cy

Where is the supercritical fluid on the phase diagram?

V V Brazhkin, A G Lyapin, V N Ryzhov, K Trachenko, Yu D Fomin, E N Tsiok

DOI: 10.3367/UFNe.0182.201211a.1137

Contents

Abstract. We discuss the fluid state of matter at high temperature and pressure. We review the existing ways in which the boundary between a liquid and a quasigas fluid above the critical point are discussed. We show that the proposed 'thermodynamic' continuation of the boiling line, the 'Widom line', exists as a line near the critical point only, but becomes a bunch of short lines at a higher temperature. We subsequently propose a new 'dynamic' line separating a liquid and a gas-like fluid. The dynamic line is related to different types of particle trajectories and different diffusion mechanisms in liquids and dense gases. The location of the line on the phase diagram is determined by the equality of the liquid relaxation time and the minimal period of transverse acoustic excitations. Crossing the line results in the disappearance of transverse waves at all frequencies, the diffusion coefficient acquiring a value close to that at the critical point, the speed of sound becoming twice the particle thermal speed, and the specific heat reaching $2k_B$. In the high-pressure limit, the temperature on the dynamic line depends on pressure in the same way as does the melting temperature. In contrast to the Widom line, the proposed dynamic line separates liquid and gas-like fluids above the critical point at arbitrarily high pressure and temperature. We propose calling the new dynamic line the 'Frenkel line'.

V V Brazhkin, V N Ryzhov L F Vereshchagin Institute for High Pressure Physics, Russian Academy of Sciences, 142190 Troitsk, Moscow, Russian Federation
E-mail: brazhkin@hppi.troitsk.ru, ryzhov@hppi.troitsk.ru;
Moscow Institute of Physics and Technology, Institutskii per. 9, 141700 Dolgoprudnyi, Moscow region, Russian Federation
A G Lyapin, Yu D Fomin, E N Tsiok
L F Vereshchagin Institute for High Pressure Physics, Russian Academy of Sciences, 142190 Troitsk, Moscow, Russian Federation
E-mail: brazhkin@hppi.troitsk.ru, alyapin@hppi.troitsk.ru, ryzhov@hppi.troitsk.ru, fomin314@mail.ru, elena.tsiok@gmail.com
K Trachenko South East Physics Network and School of Physics, Queen Mary University of London, Mile End Road, London, E1 4NS, UK
E-mail: k.trachenko@qmul.ac.uk

Received 20 September 2011, revised 31 October 2011
Uspekhi Fizicheskikh Nauk **182** (11) 1137 – 1156 (2012)
DOI: 10.3367/UFNr.0182.201211a.1137
Translated by S N Gorin; edited by A Radzig

1. Introduction

Many of the terms in physics are determined not so rigorously as those used in mathematics. In most cases, the use of insufficiently rigorous terms and definitions does not lead to serious difficulties; it is only sufficient that the expressions that relate various physical quantities be true. At the same time, in some cases, at a certain stage it is required that the terminology be refined in order to clarify the picture of a physical phenomenon.

The term 'fluid' is usually utilized to determine a flowable state of a substance that does not retain its shape, i.e., it is applicable to both a liquid and a gas. A liquid is a condensed state of a substance, i.e., in contrast to a gas, it retains its volume, it has a free surface, and at low temperatures it is capable of sustaining a negative pressure (uniform tension). Upon heating in some range of pressures, the liquid undergoes a first-order phase transition into a gas phase. The curve of the liquid–gas phase equilibrium on the $P-T$ plane ends at a critical point. At pressures and temperatures exceeding the critical values ($P > P_c$, $T > T_c$), the properties of the substance in the isotherms and isobars change continuously; the substance in this case is assumed to be in the state of a supercritical fluid, in which there is no difference between the gas and the liquid [1]. A supercritical fluid can be considered as a strongly compressed gas or as a liquid with a reduced

density (the density of the liquid near the critical point is a factor of 2–3.5 less than the density of this liquid at low temperatures and pressures near the triple point). The viscosity and the diffusion coefficients in a supercritical fluid occupying the region near the critical point have values that are intermediate between those typical of the liquid and the gas.

For most substances, the pressures and temperatures corresponding to the state of a supercritical fluid are hard to achieve; therefore, investigations of supercritical fluids were limited for a long time. In recent decades, however, a true boom has occurred in the investigation of this exotic state of substance. From the physical point of view, of most interest is the $P-T$ region near the critical point, where the so-called anomalous behavior is observed, i.e., anomalously strong dependences of the majority of physical properties on the temperature and pressure. For metals, the behavior of the physical properties is complicated by the electron subsystem and Coulomb interaction effects; in particular, a metal–insulator transition occur near the critical point [2].

An additional stimulus for investigations of the properties of fluids in recent years has been the wide industrial application of 'supercritical' technologies. Supercritical fluids are extremely strong solvents and are widely used for waste processing, extraction (in chemistry and pharmacology), as reaction media, etc. [1]. The leader in the industrial application of supercritical fluids is carbon dioxide, CO_2, since this compound can relatively easily be transferred to a supercritical state ($P_c = 73$ atm, $T_c = 31\,^\circ$C); in addition, CO_2 is inexpensive and nontoxic. The wide technological application of supercritical fluids, especially in chemistry and biology, has led to the necessity of a thorough investigation of the supercritical state of the substances. *The Journal of Supercritical Fluids* — a journal that is completely devoted to the study of the properties of fluids and to their application — has been issued since 1988. Several thousand papers concerning this research area have been published. At the same time, it is not completely clear how, even if not rigorously but at least constructively, to determine the region on the phase diagram were a supercritical fluid exists.

2. Supercritical fluid

In standard equilibrium $P-T$ phase diagrams of substances there are regions of stability of three aggregate states — solid, liquid, and gaseous — separated by phase boundaries. Most frequently, the region of supercritical fluid in a schematic phase diagram is assumed to lie for $T > T_c$ and $P > P_c$ [3] (Fig. 1a). There are also some other definitions of the field of existence of the supercritical fluid, e.g., as a region located for only $T > T_c$ or for only $P > P_c$, or as a region in which any of these conditions are fulfilled ($T > T_c$ or $P > P_c$). In any case, the line of the first-order phase transition (boiling curve) does not fall into the region of the supercritical fluid. It is also unclear where the region of existence of the 'true' liquid phase is located. Sometimes, it is assumed that the region of the liquid phase is that part of the phase diagram lying above the melting curve, where the conditions $P < P_c$ and $T < T_c$ are fulfilled simultaneously, while the remaining part of the liquid-phase region located for $P > P_c$ is called undercritical fluid.

Many researchers, naturally, understand the conditional character of the term 'supercritical' fluid and schematically depict the region of its existence near the critical point (Fig. 1b). There is a certain reason for such an approach, since most properties of substances have anomalously strong

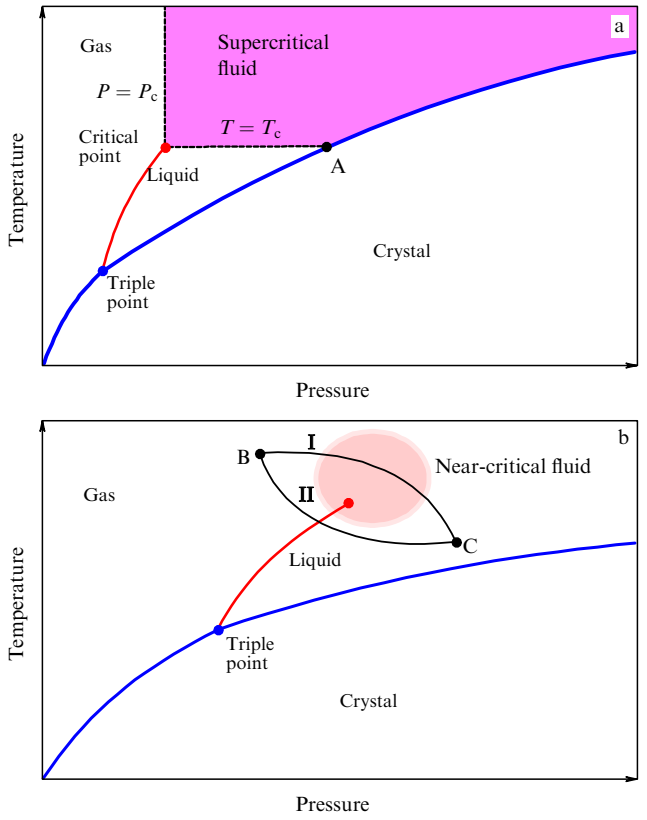

Figure 1. (a) Traditionally accepted region of supercritical fluid limited by the critical isotherm and isobar in the crystal–liquid–gas phase diagram. Point A, which is determined by the intersection of the critical isotherm and melting curve, is not a physically preferred point in the melting curve. (b) Region of near-critical fluid in the phase diagram and the illustration of the well-known fact that between two points in gas and liquid (B and C) there are always paths with a continuous variation of properties (path I) and paths that pass through the boiling curve (path II).

temperature and pressure dependences just near the critical point, in the so-called critical region. For most real substances, the conditional size of the critical region does not exceed several dozen percent, as compared to the values of T_c and P_c. In our opinion, it is more reasonable to call such a region the near-critical fluid, since the critical behavior of the properties of substances near the critical point is also observed for $T < T_c$ and $P < P_c$.

In reality, such definitions of the region of existence of supercritical fluid are not only unconstructive but also frequently lead to wrong conclusions. All these definitions implicitly suggest that the parameters P and T change along the isotherms or isobars; in this case, for $T > T_c$, $P > P_c$ the gas–liquid transition line is not intersected, i.e., all properties of the substance vary continuously. At the same time, it is obvious that for any points on the $P-T$ plane in the region of stability of liquid and gaseous phases there are trajectories connecting these points which both intersect and do not intersect the line of the phase transition (Fig. 1b). The schematic representation of the region of stability of the supercritical fluid in the phase diagram shown in Fig. 1a is not too constructive, first of all, since the structure and properties of fluids change far from the critical point quite smoothly. For example, no difference exists near the melting curve in the structure and properties of the fluid along the melting curve on different sides of point A in Fig. 1a (the point of intersection of the melting curve and the $T = T_c$ line). In

addition, to the right of point A the $T = T_c$ line lies in the region of stability of the crystalline phase, i.e., for the supercritical fluid to exist, it is necessary that not only the condition $T > T_c$ but also the condition $T > T_m$ (where T_m is the melting point) be fulfilled. In real substances, this point lies in the region of superhigh pressures ($P \gg P_c$); for example, point A in Fig. 1a for argon lies at $P \approx 60P_c$, and for water at $P \approx 300P_c$. Correspondingly, in the isotherms for $T \gg T_c$, the fluid shows no qualitative changes in the structure and properties when the line $P = P_c$ intersects.

At first glance, the problem concerning the location of the region of the state of the supercritical fluid in the phase diagram seems to be forced and purely terminological. However, this is by no means the case: the problem of the existence of a conditional boundary between the supercritical fluid and 'true' liquid for $P > P_c$ does exist in reality. This is related primarily to the fact that the conceptions concerning the nature of the liquid state changed noticeably to the end of the 20th century.

In the first half of the 20th century, beginning from the van der Waals model, approaches in which liquid was considered as a dense nonideal gas predominated. To a significant extent, these approaches (although already in a modern mathematical language) serve to date as a basis for the theory of liquids [4]. At the same time, it has become understood in recent decades that near the melting point liquids have much more in common with solids than with gases. The density of liquids is much closer to that of solids and, in spite of the absence of long-range order, liquids are characterized by a rather clearly pronounced short-range order. The zero value of the shear modulus of liquids, which is responsible for their fluidity, takes place only at low frequencies. At sufficiently high frequencies, liquids behave like solids: they have a 'solid-like' spectrum of excitations, moduli of shear elasticity close to 'solid-like' ones, etc. [5–10]. As a result, many physical quantities (heat capacity, thermal conductivity, electrical conductivity, etc.) change only slightly upon the melting of a crystal, in spite of the loss of long-range order. The vitrification of liquids upon sufficiently rapid cooling also reflects the proximity of the solid and liquid states. Glasses at low temperatures are solids and differ from crystals only in the absence of long-range order in their structure. The continuous transition of liquids into glasses with decreasing temperature indicates the existence of solid-like properties in melts on small time scales. Thus, there is a certain 'dyarchy' in the physics of the liquid state: in the majority of first-principles approaches, liquids are considered as a dense gas with a moderately strong particle–particle interaction, whereas numerous experimental facts point to a genetic affinity of the liquid and solid states. No consistent first-principles theory of such solid-like liquids has been developed so far; there are only various empirical approaches [11–13].

A vivid manifestation of the solid-like properties of liquids was the discovery of phase transformations in melts [14, 15]. It turned out that substances in a liquid state at various temperatures and pressures can have radically different short-range-order structures and, correspondingly, markedly different properties [14]. Sharp or smeared phase transformations between the different states (phases) of one and the same liquid, which are analogous to phase transformations between different crystalline phases, can occur with changes in the parameters P and T. Obviously, such a behavior of liquids agrees poorly with the conception of a liquid state as that of a condensed structureless gas.

The specificity of the structure of liquid metals, liquid semiconductors, and network covalent melts was recognized quite long ago; at the same time, liquid rare gases and simple molecular liquids had, until recently, been considered as quasigaseous fluids. However, it has been established in recent years that these liquids at temperatures close to their melting points also have a solid-like spectrum of acoustic excitations in the case of small wavelengths and have a certain short-range-order structure [16, 17].

In recent decades, regions of superhigh pressures ($P \gg P_c$) and high temperatures ($T > T_c$) have become accessible for experimental investigations (i.e., the regions of stability of the liquid state to the right of point A along the melting curve in Fig. 1a). The corresponding pressures for liquid rare gases and simple molecular substances are on the order of several kilobars; for metals and covalent substances, they are several hundred kilobars. For many substances, the transformations between different liquid modifications occur precisely in such a region. This is the case, for instance, for liquid phosphorus [18, 19]; therefore, the authors of paper [19] supposed that the phase transformation in liquid phosphorus is a transition between a supercritical molecular fluid and the liquid high-pressure phase of phosphorus. In reality, the phase transition in liquid phosphorus near the melting curve occurs in the region that is quite far from the critical point ($P \sim 1$ GPa $\approx 120P_c$, and $T \sim 1300$ K $\approx 1.3T_c$). It is obvious that the state of liquid phosphorus at these parameters hardly resembles the state of a supercritical fluid near the critical point. It was, for example, established that the structure of the liquid argon near the melting curve does not change qualitatively with increasing temperature up to $T \sim 4T_c$, and to pressures $P \sim 10^3 P_c$ [17], which means that the consideration of the state of liquid phosphorus for $P > 100P_c$ and $T > T_c$ as a supercritical fluid that was suggested in paper [19] appears to be wrong.

In the case of an isobaric increase in temperature at pressures exceeding the critical value, the density of a liquid decreases, and at sufficiently high temperatures the liquid becomes similar to a dense structureless gas. A further heating leads in real substances to their partial ionization and a transition into a plasma state at temperatures of $10^4 - 10^6$ K, whereas an increase in the liquid temperature is not formally restricted in the case of model systems of particles. It can be supposed that in the $P-T$ and $\rho-T$ phase diagrams (ρ is the density of the substance) a line (or a narrow band) should be observed that separates the state of the 'true' liquid with a solid-like spectrum of excitations and with clearly pronounced short-range-order peculiarities from the state of a supercritical fluid with a random-packing structure. Therefore, the question concerning the place of the quasigaseous supercritical fluid in the phase diagram, including its place at superhigh pressures ($P \gg P_c$), is quite reasonable.

3. 'Thermodynamic' extrapolation of the boiling curve: Widom line

3.1 Hypercritical 'ridges' of thermodynamic anomalies

A rather obvious but, as we show below, not too constructive approach to the solution to this problem is the consideration of the lines of thermodynamic anomalies in the hypercritical region. Indeed, an anomalous behavior of most of the thermodynamic characteristics is observed at temperatures and pressures exceeding critical values.

The correlation length ξ for thermodynamic fluctuations diverges at the critical point [20]. Near the critical point, a critical behavior of physical quantities that are determined by the second derivatives of the Gibbs thermodynamic potential is observed; for example, the compressibility coefficient β_T, thermal expansion coefficient α_P, and heat capacity c_P go through maxima upon varying pressure or temperature. All these quantities near the critical point are proportional to a power function of the correlation length ξ, and the positions of their maxima on the $P-T$ plane are close to each other [20, 21]. This is also the case for the density fluctuations $\zeta_T = \langle (\Delta N)^2 \rangle / \langle N \rangle \sim (\partial\rho/\partial P)_T$, where $(\partial\rho/\partial P)_T$ is the derivative of the density with respect to pressure at a constant temperature.

Thus, there is a whole set of 'lines of maxima' of various thermodynamic quantities in the hypercritical region, and all these lines merge asymptotically into a single line when approaching the critical point. Each of these lines can be considered as a continuation of the line of liquid–gas phase equilibrium. Smearing of the maxima of each of these quantities and the maxima's diminishing in height form something resembling a mountain ridge; so, these lines of maxima were called 'ridges' [22–24].

Information on the positions of ridges on the $P-T$ plane is quite important; in particular, the positions of the ridges determine the maxima of such important technological characteristics as the dissolving capacity of a supercritical fluid, and the rates of chemical reactions in the fluid, etc. [1]. It turned out that the experimentally determined lines of ridges are close to isochore and exhibit a moderate decrease in density with increasing temperature; the divergence between the lines of the different ridges and the isochore increases when moving away from the critical point [22–24]. Most investigations of the hypercritical region have been focused on studies of ridges connected with the density fluctuations [22].

Stanley [21] suggested that the line of the maxima of the correlation length of fluctuations in the isotherms be called a 'Widom line'. Since the lines of maxima near the critical point merge in fact into a single line, it was suggested that this name be used in a wider sense, for designating lines of maxima of any quantities that are determined by the second derivatives of the Gibbs thermodynamic potential. It should be noted that Benjamin Widom himself does not consider the lines of hypercritical anomalies as some special lines. In the literature, a Fisher–Widom line, which separates two modes of attenuation of spatial correlations in liquids [25], and the symmetry line in the lattice model of the liquid [26] are encountered more frequently. Nevertheless, since Widom contributed so much to the development of the theory of critical phenomena, Stanley suggested that the line of maxima of the correlation length be called the Widom line in his honor.

Stanley and colleagues [27, 29, 30] and Artemenko et al. [28] also noted that similar lines should exist in the case of liquid–liquid transformation if such a transformation is a first-order phase transition ending in a critical point at high temperatures. Notice that the 'thermodynamic' continuations of the lines of liquid–liquid transitions are quite reasonable. It is precisely the Widom lines for the liquid–liquid transformations that correspond to the maximum of fluctuations between two types of short-range orders. The authors of Ref. [21] supposed that the dynamics of particles in liquids should also change qualitatively near the Widom line. It should be noted that such lines will also occur as extensions of lines of isomorphic transitions in crystals into the hypercritical region, for example, for the $\gamma-\alpha$ transition in crystalline Ce.

Computer simulations with the use of various interaction potentials between particles make it possible to establish that we may speak of a sufficiently definite Widom line for the liquid–liquid transition only in the case of temperatures and pressures that exceed the critical values by no more than a few dozen percent [27–30]. At greater distances from the critical point, the ridges for different quantities diverge and can be observed both experimentally and in computer simulation at temperatures of up to $(1.5-2)\,T_c$. A systematic investigation of the behavior of the maxima of various quantities for liquid–gas transitions in the hypercritical region was performed in our recent work [31, 32].

3.2 Widom lines for a van der Waals fluid and for a fluid of Lennard-Jones particles

One of the simplest and most known equations of state for fluids is the van der Waals equation, which in the reduced variables $T_r = T/T_c$, $P_r = P/P_c$, and $\rho_r = \rho/\rho_c$ is written down as

$$(P_r + 3\rho_r^2)(3 - \rho_r) = 8T_r\rho_r\,. \tag{1}$$

The properties of the van der Waals equation have been studied quite well: analytical expressions have been obtained in this model for the majority of the thermodynamic characteristics of liquids and gases in the region below the critical point [33]. At the same time, as strange as this can seem, the behavior of the van der Waals model of the fluid in the hypercritical region of the P and T parameters has been studied insufficiently. In terms of the van der Waals model, it is not a very complex problem to obtain analytical expressions for the lines of hypercritical anomalies [32]. Earlier, Nishikawa et al. [22] analyzed the behavior of the line of maxima of density fluctuations:

$$\frac{\langle \Delta N^2 \rangle}{\langle N \rangle} = k_B T \left(\frac{\partial\rho}{\partial T} \right)_T \equiv \zeta_T\,.$$

It has been established that the position of the line of maxima of the density fluctuations on the isotherms satisfies the equation

$$\rho_r = 3 - 2T_r^{1/3}\,, \tag{2}$$

and that this line ends at the zero density and zero pressure at $T = 3.375T_c$ (Fig. 2). In Ref. [22], an erroneous assumption was made that the maxima of other thermodynamic quantities on the isotherms should lie approximately on the same line. In reality, as will be shown below, all the ridges diverge already at an insignificant distance from the critical point.

The isothermal compressibility in the van der Waals model is written as

$$\beta_T = \rho^{-1} \left(\frac{\partial\rho}{\partial P} \right)_T = -\frac{(\rho_r - 3)^2}{6\rho_r\left[-4T_r + \rho_r(\rho_r - 3)^2 \right]}\,.$$

The line of maxima of the compressibility β_T obeys the equation

$$T_r = \frac{\rho_r(3 - \rho_r)^3}{2(3 + \rho_r)} \tag{3}$$

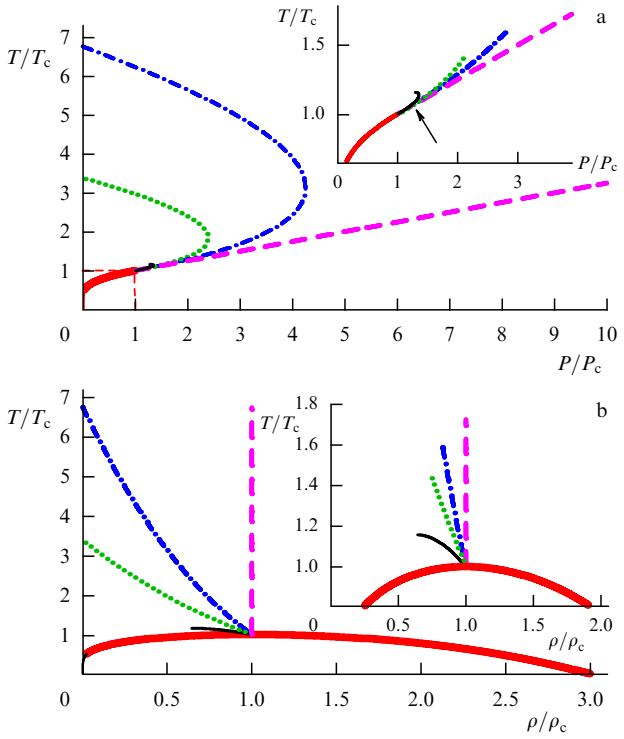

Figure 2. (a) $P-T$ and (b) $\rho-T$ phase diagrams for a van der Waals liquid, which display theoretically calculated lines of maxima of specific heat c_P (dashed line), thermal expansion coefficient α_P (dashed–dotted line), thermal fluctuations ζ_T (dotted line), and compressibility β_T (thin solid line). The thick solid line corresponds to the liquid–gas boundary. The insets show enlarged parts of Figs 2a and 2b, where the corresponding lines end at the points at which the quantity changes in the isotherms within 1%. The arrow in the inset to Fig. 2a indicates the point below which all four lines of the maxima converge (with an accuracy not worse than 1%) into a single Widom line.

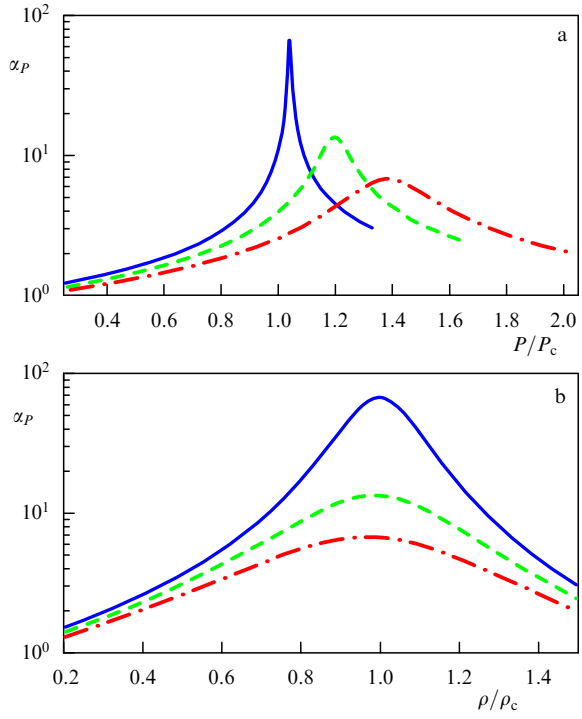

Figure 3. Dependence of the thermal expansion coefficient α_P on (a) the pressure, and (b) the density for a van der Waals system at temperatures $T/T_c = 1.01$ (solid line), $T/T_c = 1.05$ (dashed line), and $T/T_c = 1.1$ (dashed–dotted line).

and ends at its own 'critical' point: it disappears at $T_r = 1.1556$, $P_r = 1.2848$, and $\rho_r = 0.64575$ (see Fig. 2). The line of maxima of the heat capacity c_P coincides with the isochore $\rho_r = 1$ and in the (P, T) coordinates is described by the equation

$$T_r = \frac{3}{4} + \frac{1}{4} P_r , \qquad (4)$$

thus being a direct continuation of the line of the gas–liquid equilibrium [33] (see Fig. 2). The thermal expansion coefficient is written down as

$$\alpha_P = -\frac{1}{\rho}\left(\frac{\partial\rho}{\partial T}\right)_P = \frac{4(\rho_r - 3)}{3\rho_r(\rho_r - 3)^2 - 12T_r} .$$

The line of maxima of the thermal expansion coefficient α corresponds to the equation

$$T_r = \frac{(3 - 2\rho_r)(3 - \rho_r)^2}{4} . \qquad (5)$$

Similar to the line of maxima of density fluctuations, this line ends at zero pressure and zero density at $T = 6.75T_c$ (see Fig. 2).

Although all lines of maxima are described by different equations, they are close to one another in the vicinity of a critical point. For estimations, all lines of extrema can be assumed to be coincident if the values of the temperature in lines at the same pressure differ by no more than 1%, which approximately corresponds to the accuracy of measurements of the corresponding quantities and to the errors in the results of numerical simulations. For a van der Waals fluid, the extrema of different thermodynamic quantities merge, in fact, into a single Widom line only for $T < 1.07T_c$ and $P < 1.25P_c$ (Fig. 2a). Notice that the analytical expressions that were obtained for the lines of hypercritical anomalies in the van der Waals model are of independent interest as well [32].

Although for the van der Waals fluid the lines of maxima of the density fluctuations and of the maxima of the thermal expansion coefficient extend formally up to zero pressures, and the line of maxima of the heat capacity goes formally into the region of infinite temperatures, the amplitudes of all maxima fall off quite rapidly upon moving away from the critical point (Figs 3, 4). As a conditional criterion for the actual disappearance of a maximum, it is suitable to consider the ratio of the corresponding thermodynamic quantity in the maximum to the magnitude of this quantity at a density that differs by 10% from the density in the maximum. If this ratio is less than 1.01 (the excess of the maximum over the background is less than 1%), the ridge can be assumed to be actually smeared. When using this criterion, the lines of all maxima, in fact, end at relatively small temperatures and pressures (see Fig. 2):

$$T_r \sim 1.59 , \quad P_r \sim 2.78 , \quad \rho_r \sim 0.83 \quad \text{for} \quad \alpha_P ,$$

$$T_r \sim 1.44 , \quad P_r \sim 2.13 , \quad \rho_r \sim 0.74 \quad \text{for} \quad \zeta_T ,$$

$$T_r \sim 1.73 , \quad P_r \sim 3.9 , \quad \rho_r \sim 1 \quad \text{for} \quad c_P .$$

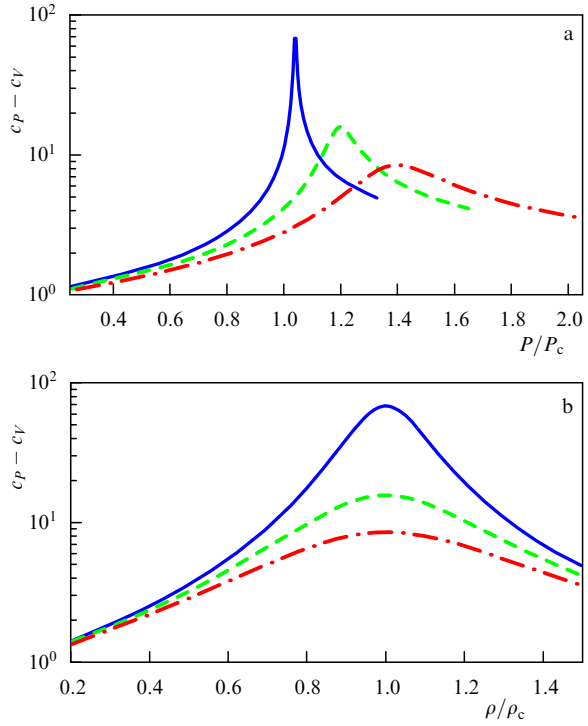

Figure 4. Dependence of the difference of the specific heats $c_P - c_V$ on (a) the pressure, and (b) the density for a van der Waals system at temperatures $T/T_c = 1.01$ (solid line), $T/T_c = 1.05$ (dashed line), and $T/T_c = 1.1$ (dot-and-dash line).

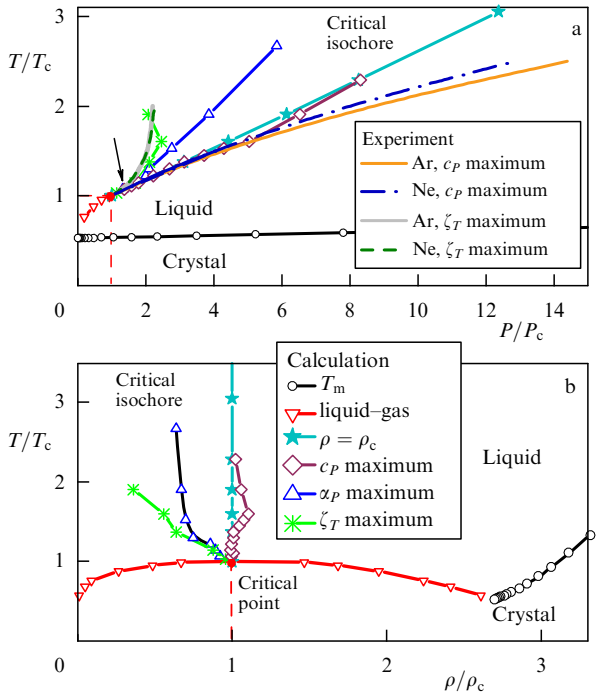

Figure 5. (a) $P-T$ and (b) $\rho-T$ phase diagrams for a system of particles interacting via a Lennard-Jones potential. The calculated lines are given for the maxima of specific heat c_P, thermal expansion coefficient α_P, thermal fluctuations ζ_T, and compressibility β_T as against the experimental data for Ar and Ne. All simulated dependences are represented by symbols at the points of calculations with interpolation lines between them (the designations are identical for both diagrams). The simulated lines of maxima are continued to the sites where they can be determined from calculations. The arrow in Fig. 5a indicates the point below which all three lines join (with an accuracy not worse than 1%) into a single Widom line.

It is interesting that in the van der Waals model the lines of maxima of thermodynamic quantities correspond to a decrease in the density with increasing temperature (Fig. 2b), and only the line of maxima of the specific heat c_P lies on the isochore. According to paper [22], the physical cause of the fact that the lines of maxima of density fluctuations and of maxima of the correlation length ξ correspond to a decrease in the density is related to an increase in the effective volume 'captured' by the molecules with increasing temperature.

Let us now consider the lines of maxima of different physical quantities in the hypercritical region for a system of particles with a Lennard-Jones interaction potential

$$U(r) = Ar^{-12} - Br^{-6}\,.$$

It is well known that the Lennard-Jones potential well reproduces the behavior of many molecular substances and rare gases. The thermodynamic and kinetic properties of a system of Lennard-Jones particles have been studied using computer simulation in thousands of papers; however, a systematic analysis of the behavior of thermodynamic quantities in the hypercritical region has been performed only recently [31, 32].

The behavior of the maxima of β_T, α_P, c_P, and ζ_T quantities has been calculated (see Appendix). The results are summarized in Fig. 5. With increasing temperature and pressure, the maxima of all these quantities decrease rapidly and become smeared (Figs 6, 7). The criterion of the almost complete disappearance of the maxima was chosen in the same way as earlier for the van der Waals model. Figure 5a also shows the experimental positions of the maxima for c_P and ζ_T for argon and neon [34]. The maxima of β_T, α_P, c_P, and ζ_T are traced with increasing temperature up to $T_r < (2-2.5)$. The temperatures of the 'ends' of the lines of maxima are $\sim 1.1T_c$ for β_T, $\sim 2T_c$ for ζ_T, $\sim 2.8T_c$ for α_P, and $\sim 2.5T_c$ for c_P.

It is seen from Fig. 5a that the lines corresponding to the hypercritical maxima for argon and neon agree rather well with the results of numerical simulations. Qualitatively, the behavior of the lines of hypercritical anomalies is similar to that observed for the van der Waals model. Most lines correspond to a decrease in the density with increasing temperature, and only the line of maxima of the heat capacity c_P lies close to the isochore and somewhat deviates toward greater densities for $T_r > 2$.

Summing up, it may be concluded that the thermodynamic continuation of the line of gas–liquid phase equilibrium represents a single line at a distance from the critical point equal to only several dozen percent in temperature and pressure, and upon moving further from the critical point it transforms into a rapidly expanding bunch of lines, which adjoins the isochore on the side of low densities and ends at $T_r \sim 2-2.5$ and $P_r \sim 10-15$.

The quantities ζ_T and β_T are related to the definition of the correlation length ξ [20]:

$$\left(\frac{R}{\xi}\right)^2 = (\rho k_B T \beta_T)^{-1}\,,$$

where R is the Debye attenuation length estimated as

$$R^2 \sim \int \mathrm{d}r\, r^2 C_2(r, T)\,,$$

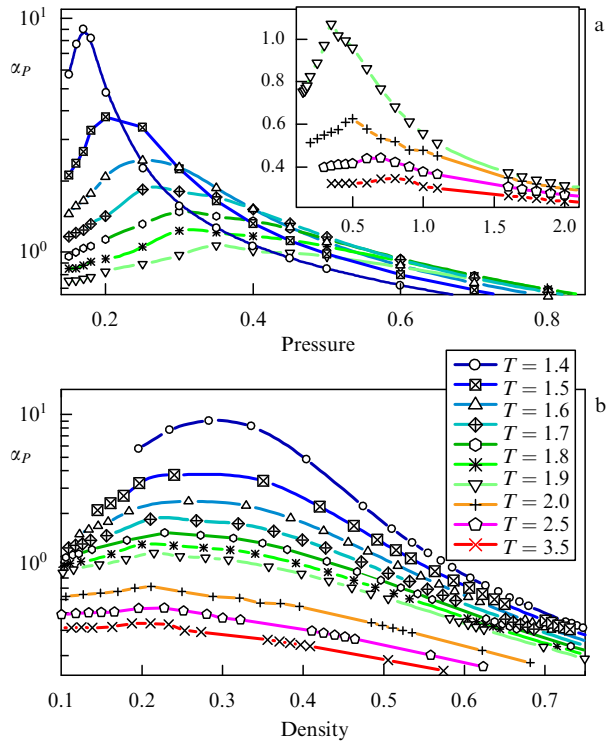

Figure 6. Dependence of the thermal expansion coefficient α_P on (a) the pressure, and (b) the density for a system of particles with a Lennard-Jones potential at various temperatures. The inset to figure 6a displays the $\alpha_P(P)$ dependences at high temperatures. The values of the temperature shown in the inset to figure 6b are common to figures (a) and (b). All data are given in Lennard-Jones units.

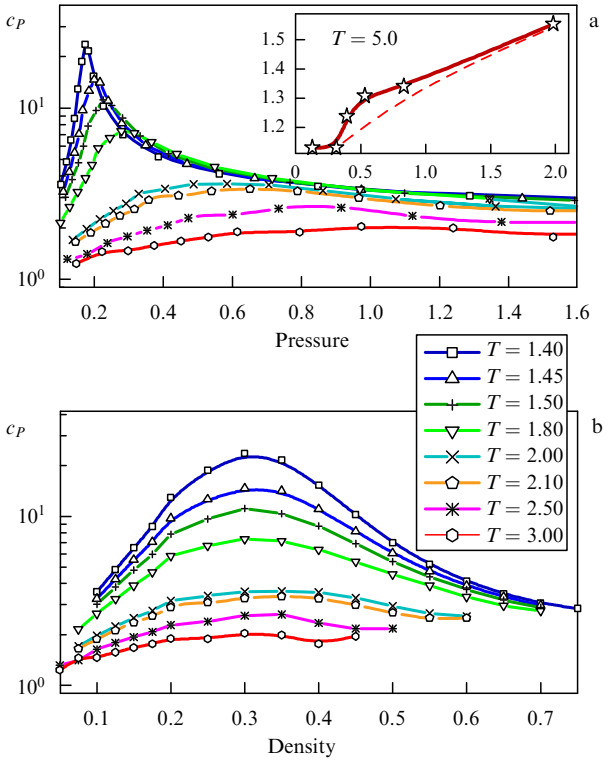

Figure 7. Dependence of the specific heat c_P on (a) the pressure, and (b) the density for a system of particles with a Lennard-Jones potential at various temperatures. The inset to Fig. 7a displays (as an example) a high-temperature curve whose maximum cannot be determined. The temperatures shown in the inset to Fig. 7b refer to both figures (a and b). All data are given in Lennard-Jones units.

and $C_2(r, T)$ is the direct correlation function. It is hardly possible to restore the position of the line of maxima of the correlation length even in terms of the van der Waals model. Usually, it is assumed that the isotherms of the correlation length behave like those of the density fluctuations [22]. The correlation length, which is related to density fluctuations, is determined from the expression [20]

$$\big\langle \big(\rho(0) - \rho\big)\big(\rho(r) - \rho\big)\big\rangle \sim \frac{\exp\left(-r/\xi\right)}{r}\,. \tag{6}$$

The complicated dependence of ξ on the volume cannot be obtained analytically; it strongly depends on the approximations accepted. The position of the maximum of the quantity ξ in the isotherm depending on the volume is even more sensitive to the approximations involved and to the procedure of achieving self-consistency. In any case, the line of maxima of ξ lies inside the bunch of the other lines and, in fact, ends at $T_r \sim 2$.

Thus, the idea of the 'thermodynamic' extension of the liquid–gas equilibrium curve with the aim of conditionally separating a 'true' liquid from a supercritical fluid at superhigh pressures ($P \gg P_c$) does not prove its value. The thermodynamic continuation in reality represents a rapidly expanding region ending at $P \sim (10-15)\,P_c$. In fact, this bunch of lines lies inside the region of 'near-critical' fluid shown in Fig. 1b.

Recently, Simeoni et al. [35] have undertaken an attempt to extrapolate the Widom lines for argon into the region of superhigh pressures on the basis of experimental data on the positions of the maximum of heat capacity c_P in the isotherms. As was already said above, the maxima of c_P actually become completely smeared for $T_r > 2.5$, and the allowance for such conditional maxima performed in the range of $2.5 < T_r < 3.1$ made in Ref. [35] is incorrect. A slight deviation of the line of maxima of c_P into the region of greater densities at high temperatures for both a Lennard-Jones liquid and for real fluids (Ar, Ne; see Fig. 5a) is related to the fact that far in the hypercritical region the quantity c_P itself increases with increasing pressure (see inset to Fig. 7a). As a result, the position of a smeared maximum of a small height is shifted effectively into the region of higher densities and pressures.

In any case, the extrapolation of this curve into the region of superhigh pressures ($P_r \sim 100$) that was performed in paper [35] makes no sense, since for $P_r > 20$ there are no thermodynamic anomalies, and the Widom line (or bunch of lines) ends there.

3.3 Batschinski separatrix

Concluding the consideration of special lines of 'thermodynamic origin' in the phase diagram of fluids, it is necessary to mention one more important curve, namely, the Batschinski separatrix, which has recently frequently been called the Zeno line [36–38]. This line corresponds to the equation

$$PV = RT\,, \tag{7}$$

i.e., to the condition of the formal coincidence of the equation of state of a fluid with the equation of state of an ideal gas. A I Batschinski [36] was first to show that in terms of the van der Waals model this line is straight in the (ρ, T) coordinates. From the physical point of view, moving along this line reflects the formal compensation of the attraction and

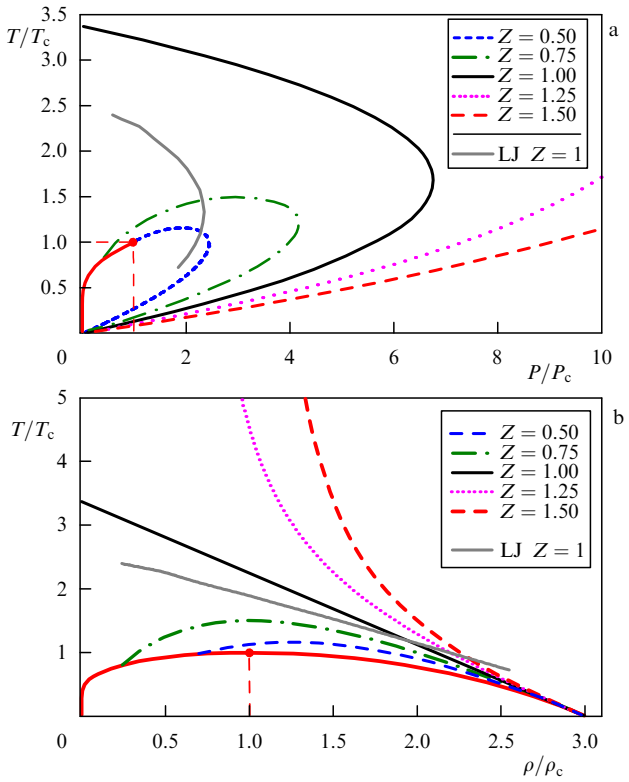

Figure 8. Batschinski separatrix $PV/(RT) \equiv Z = 1$ and other isolines $Z = \text{const}$ for a van der Waals system in the (a) $T-P$, and (b) $T-\rho$ phase diagrams. For comparison, the line $Z = 1$ is also shown for a system of particles with a Lennard-Jones potential.

repulsion potentials. In most of later work, the behavior of this line was analyzed only in the (ρ, T) coordinates for model and real systems [37–39]. At the same time, it is of interest to consider the behavior of not only the Zeno line but also other lines that are determined by the condition $PV/(RT) = \text{const}$, both on the $\rho - T$ and $P - T$ planes [32].

The equations for the lines defined by the condition $PV/(RT) = \text{const}$ for the van der Waals model have the form

$$T_r = \frac{3\rho_r(3-\rho_r)}{8-k(3-\rho_r)}\,. \tag{8}$$

Here, it should be taken into account that the condition $PV/(RT) = \text{const}$ in the given variables is written as $P_r/(\rho_r T_r) = k$, and the condition $PV/(RT) = 1$ corresponds to $k = 8/3$.

Figure 8 displays lines corresponding to the condition $PV/(RT) = \text{const}$ for a van der Waals fluid, and for a model system of particles interacting via a Lennard-Jones potential. The behavior of these lines for $PV/(RT) < 1$ and for $PV/(RT) > 1$ is quite different. The line that is determined by Eqn (7) separates two regions of the fluid: the 'soft' fluid with a low density, in which the condition $PV/(RT) < 1$ is fulfilled, and a more 'rigid' fluid with an enhanced density, in which the inequality $PV/(RT) > 1$ is kept (see Fig. 8); therefore, the line $PV = RT$ can be called a separatrix. The Batschinski separatrix is the only line from the given family of lines which ends at the zero values of the density and pressure, i.e., it is 'sewn' to that in the ideal gas model. Although the Batschinski separatrix is of independent interest and at the near-critical temperatures qualitatively separates fluid with a low (quasigas-like) density from that with an enhanced (liquid-like) density, it cannot serve as a conditional boundary between a liquid and a supercritical fluid at superhigh pressures. The Batschinski separatrix for a van der Waals fluid ends at $T = 3.375T_c$, i.e., at the same temperature as the line of maxima of density fluctuations does. This coincidence is, of course, not accidental; it is related to the circumstance that the line of maxima of density fluctuations corresponds to the zero second derivative of the density with respect to pressure. For an ideal gas, this derivative is equal to zero at all temperatures; therefore, the line of maxima of density fluctuations at the zero pressure is also sewn to with the equation of state for an ideal gas: $PV = RT$. The coincidence of the Batschinski separatrix with the line of maxima of density fluctuations at zero pressure will naturally take place for all fluids.

4. 'Dynamic' separation between a liquid and a fluid: Frenkel lines

4.1 Rigid liquids and soft fluids

Thus, to distinguish a 'true' solid-like liquid from a quasigas-like fluid at superhigh pressures, other criteria are necessary.

It turns out that, as a possible criterion, it is appropriate to consider the difference in the dynamic rather than thermodynamic characteristics of the liquid and supercritical fluid. We think that the most important point in the context of this review is that the types of trajectories of particle motion and the mechanisms of diffusion in liquids and gases are different. In gases, the kinetic energy of particles significantly exceeds the interaction energy between them, and the diffusion is determined by the free motion of particles and processes of interparticle collisions (ballistic collision-dominated regime). In liquids, the energy of interaction between the particles is relatively large at low temperatures and the diffusion process, just as in crystals and glasses, is determined by activated jumps of atoms and molecules (vibrational hopping transport). The trajectories of particle motion in liquids and gases thus have a qualitatively different character. In the time intervals between the jumps, the particle in fact vibrates near a local equilibrium position. At a temperature close to the melting point and in the supercooled liquid state, the characteristic time between particle jumps for distances comparable with interparticle distances (the relaxation time τ^* in a liquid) significantly exceeds the time of the shortest period of particle vibrations, $\tau_0 = 2\pi/\omega_0$, where ω_0 is the maximum frequency of acoustic excitations (on the order of the Debye frequency). This fact was first noted by Ya I Frenkel more than 80 years ago [11]. In recent decades, the approach in which the liquid is considered as an almost harmonic oscillating system with rather rare particle jumps has been successfully applied to the description of the thermodynamic and dynamic properties of liquids [12, 13].

As temperature increases, the relaxation time in a liquid decreases and, when it becomes comparable with the period of particle vibrations, the possibility of the time-related separation of the behavior of particles into vibrational and hopping already disappears. When $\tau^* < \tau_0$, a transition to the ballistic collision-dominated regime of diffusion occurs. Therefore, we can suppose that the condition

$$\tau^* \sim \tau_0\,, \quad \text{or} \quad \frac{\tau^*}{\tau_0} \sim 1\,, \tag{9}$$

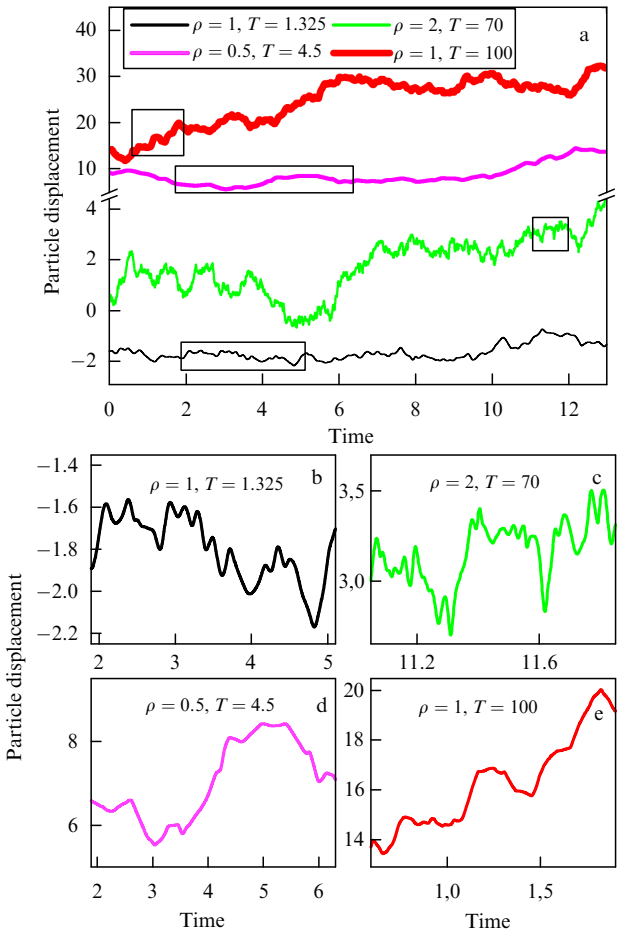

Figure 9. (a) Examples of the particle trajectories (coordinate x) for a Lennard-Jones liquid under various conditions. (b–e) Enlarged fragments outlined in figure a. In the case of (b) and (c), vibrational motion dominates in the particle motion; (d) and (e) correspond to predominantly collisional motion of particles.

corresponds to a crossover from the solid-like to quasigas-like regime of diffusion. It is precisely condition (9) that can serve as a constructive definition of a *dynamic line* separating a solid-like *rigid* liquid and a quasigas *soft* fluid at superhigh pressures [40, 41].

The definition of τ^* as the average time necessary for a particle to become displaced by an average interatomic distance extends the definition of the relaxation time in liquid — in the spirit of J C Maxwell [42] and Ya I Frenkel [11] — to the quasigas regime of diffusion, in which no vibrational motion of a particle between the jumps occurs.

The characteristic trajectories of particle motion for various regimes are displayed in Fig. 9. Naturally, the transition from the vibrational-hopping mechanism of particle motion in liquids to the collisional one is rather smeared in temperature; in reality, a smooth crossover occurs from one regime to the other. However, as is shown below, condition (9) not only determines the change in the type of trajectories of the particle motion, but also corresponds to a qualitative change in the elastic, dynamic, and thermodynamic characteristics of the liquid.

It should be noted that the following formula is frequently used for the estimation of τ^*:

$$\tau^* \sim \tau_0 \exp\left(\frac{E_{\rm act}}{k_{\rm B}T}\right), \qquad (10)$$

where $E_{\rm act}$ is the activation energy for a particle jump, and $k_{\rm B}$ is the Boltzmann constant. According to formula (10), the inequality $\tau^* > \tau_0$ is valid at finite values of $E_{\rm act}$ and arbitrary temperatures. However, at high temperatures, when the magnitude of $k_{\rm B}T$ becomes significantly larger than the height $E_{\rm act}$ of the barrier for the particle jump, expression (10) is already inapplicable. Note that the activation energy is determined by the potential energy of particle interaction; therefore, the transition to the quasigas regime of diffusion should occur when the kinetic thermal energy K of particles becomes comparable with the potential energy of their interaction:

$$\frac{3k_{\rm B}T}{2} \sim E_{\rm pot}\,. \qquad (11)$$

For most substances, the kinetic to potential energy ratio $K/E_{\rm pot}$ at the melting temperature is substantially less than unity. The particles, in this case, reside mainly in the region of the action of the potential, and upon melting relatively long-lived regions with a clearly pronounced short-range order are retained. We will return to this point in Section 4.7.

As was noted earlier, a liquid at temperatures close to the melting point has a finite value of the shear modulus and a solid-like oscillation spectrum at high frequencies [5–10, 43, 44]. Transverse-phonon type oscillations exist in liquids at frequencies exceeding the value of the inverse relaxation time: $\omega > \omega^* = 2\pi/\tau^*$. Certainly, these oscillations are strongly anharmonic and formally have a high damping coefficient. When the relaxation time becomes comparable to the minimum time τ_0 of vibrations, this condition cannot be fulfilled, since only frequencies $\omega < \omega_0$ are possible in liquids, and even the most short-wavelength transverse oscillations are lost from the oscillation spectrum of liquids for $\tau^* < \tau_0$. When $\tau^* < \tau_0$, the shear modulus of the substance is equal to zero at all frequencies $\omega < \omega_0$ possible in liquids. At higher frequencies, $\omega > 2\pi/\tau^* > \omega_0$, the shear modulus will formally remain finite, but the natural transverse vibrations, which are possible only at frequencies $\omega < \omega_0$, will be absent in the fluid. It should be noted that *the zero value of the static shear modulus is frequently considered as the main criterion for the difference between the liquid state and the solid state. The zero value of the shear modulus, but now in the entire spectrum of possible frequencies, is the main feature that distinguishes the soft fluid from the rigid liquid.*

Condition (9) indicates the proximity of the values of τ^* and τ_0. In reality, there is a rather wide distribution of both quantities, and the case at hand is an approximate equality (to an accuracy of a few dozen percent) of the average values of τ^* and τ_0. If a particle undergoes only one–two vibrations between the jumps, it is difficult to correctly determine the magnitude of τ_0, and the resolving of motion into vibrational and hopping regimes becomes impossible. At the same time, the spectrum of natural excitations of the liquid is a well-definite property, and the disappearance of all excitations like transverse acoustic vibrations from this spectrum occurs in a narrow temperature range. As a result, we can quite reasonably speak of a dynamic line that separates the two mechanisms of particle motion. The minimum period of vibrations τ_0 and the change in the regime of particle motion can be determined directly from a visual analysis of trajectories obtained by computer modeling (see Fig. 9). At the same time, more reliable results can be obtained based on an analysis of autocorrelation functions of the particle

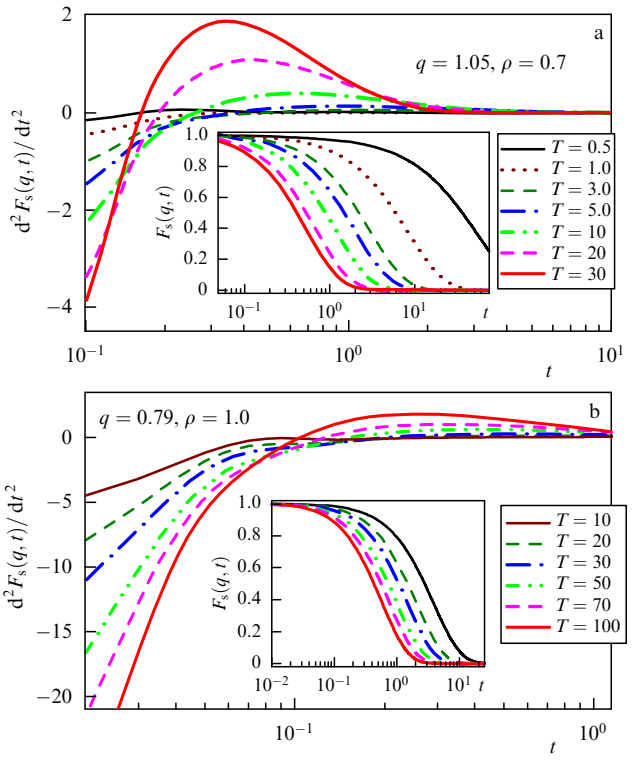

Figure 10. Second time derivatives of autocorrelation functions of dispersion (shown in the insets) for a Lennard-Jones liquid at (a) $q = 1.05$, $\rho = 0.7$, and (b) $q = 0.79$, $\rho = 1.0$. The wave vectors correspond to the maxima of structure factors. All quantities are given in Lennard-Jones units.

motion:

$$F_s(q,t) = \frac{1}{N}\left\langle \sum_{j=1}^{N} \exp\left[i\mathbf{q}\left(\mathbf{r}_j(t) - \mathbf{r}_j(0)\right)\right]\right\rangle,$$

where r_j is the radius of the jth particle.

Usually, these functions are used to analyze particle motion in viscous supercooled liquids in a state close to the vitreous state [45, 46]. However, a thorough analysis shows that the ballistic, vibrational, and collisional mechanisms of a particle motion all manifest themselves in the behavior of given correlation functions [47]. Figure 10 displays the evolution of the correlation functions for a Lennard-Jones liquid with increasing temperature along isochores. It is seen that the second derivatives of functions qualitatively change their behavior with the change in the dynamic regime of particle motion.

A phase transition, including that of a dynamic type, is, as a rule, accompanied by the divergence of some quantity at the point of transformation. Condition (9) determines a crossover in the dynamic behavior of the system. As a more rigorous criterion of the dynamic line, an analogy with percolation transitions can be used. We will discuss here the high-temperature state of fluid. Let τ^* be the time of the displacement of a given particle by an average interatomic distance. If the projection of the momentum of the particle onto the vector of its displacement changes sign at least once in this time period, such a particle will be considered to be vibrating. It is obvious that such particles will exist even in the state of a rarefied gas. The fraction of such particles grows with decreasing temperature, and at a certain temperature an infinite percolation cluster extending over the entire fluid consisting of vibrating particles arises. It can be assumed that it is precisely at this temperature that high-frequency transverse excitations arise in the excitation spectrum of the fluid.

4.2 'Fast' sound and phase transformations in rigid liquids

In many liquids, a positive dispersion of acoustic excitations is observed — an increase in the sound velocity with decreasing wavelength. This phenomenon of positive dispersion, which is sometimes called fast sound or high-frequency sound [10, 16, 35, 48], is related precisely to the crystal-like behavior of liquids at high frequencies. Ya I Frenkel predicted that the velocity of longitudinal sound in liquids at frequencies $\omega > \omega^* = 2\pi/\tau^*$ should increase from $(B/\rho)^{1/2}$ to $[(B + 4/3G)/\rho]^{1/2}$ (where B is the compressibility modulus of the liquid, and G is the shear modulus), since at high frequencies the shear modulus of liquids is nonzero [11]. For viscous liquids, this phenomenon was revealed rather long ago [6, 7]. Later on, a more rigorous theoretical basis was constructed for the description of this behavior, which was based on the formalism of 'memory functions' and the theory of coupled modes [43, 44, 49, 50]. Notice that the loss of the 'high-frequency sound' can also be revealed from an analysis of correlation functions of particle motion (see Fig. 10). It is obvious that the dynamic line determined by condition (9) establishes the upper bound of temperatures at which the phenomenon of fast sound can be observed.

For $\tau^* \gg \tau_0$, a clearly pronounced short-range order exists around each atom or molecule of the liquid in a time corresponding to many particle vibrations; when $\tau^* < \tau_0$, only random packing of particles is possible in liquids. It is precisely liquids with a definite short-range order that can undergo phase transformations under the effect of changes in pressure and temperature [14]. When describing the behavior of such liquids, it is insufficient to introduce one order parameter (density); it is also necessary to consider the local structure of the short-range order in the melt. At the same time, a quasigas-like fluid with a random packing of particles, just like a gas, is unambiguously characterized by the density. It is obvious that the phase transformations in liquids with a change in the type of short-range order can occur only at temperatures that are substantially lower than the dynamic line determined by condition (9).

4.3 Viscosity and diffusion in liquids and fluids

As follows from an analysis of data for various substances, condition (9) is fulfilled qualitatively near the critical point. In addition, it is known that liquids lose their solid-like vibrational spectrum in the vicinity of the critical point; a transition to a ballistic collisional type of particle motion is observed [51, 52]. The viscosity and the diffusion coefficient near the critical point have finite values, in contrast to the majority of other thermodynamic characteristics. It is known that all supercritical fluids possess close values of the diffusion coefficient ($D \sim 10^{-8}$ m^2 s^{-1}) and close values of viscosity [lying in the narrow range of $\eta \sim (10^{-5} - 10^{-4})$ Pa s] near the critical point. These values are intermediate between those characteristic of gases and liquids at temperatures close to the melting point. The characteristic values of the diffusion coefficient near the critical point (e.g., $D \sim 2 \times 10^{-8}$ m^2 s^{-1} for argon) are just the ones corresponding to the times of atomic jumps τ^*, which are comparable to the time τ_0 of a single atomic vibration. In this case, the diffusion root-mean-

square displacement of a particle is $\langle x^2\rangle^{1/2} \sim 1$ Å at $t \sim 10^{-12}$ s.

The relaxation time τ^* in this context can be treated as the average time of a jump to a distance equal to the interparticle spacing; consequently, this time τ^* is related to the corresponding diffusion coefficient D for liquid as

$$\tau^* \sim \frac{a^2}{6D},$$

where a is the average shortest interparticle distance. Then, condition (9) can be rewritten as

$$D \sim \frac{a^2}{6\tau_0}. \quad (12)$$

At moderate pressures $P < (5-10)\,P_c$, the compression of the fluid in the region of a soft fluid corresponding to the quasigas density (to the left from the Batschinski line) mainly occurs due to a decrease in the 'free' volume, and τ_0 changes only slightly. As the pressure increases to $10^2 P_c$, the magnitude of τ_0 changes by no more than several dozen percent, whereas the diffusion coefficient changes in the range from the melting point to the crossover temperature by several orders of magnitude (5–10 orders of magnitude for viscous liquids, and 1–2 orders for liquid rare gases). The magnitude of a^2 also changes insignificantly in the given range of pressures; in addition, both quantities, τ_0 and a^2, decrease with increasing pressure, i.e., the ratio a^2/τ_0 changes to an even smaller extent. As a result, we can choose in the initial range of pressures the line of the constant value of the diffusion coefficient ($D = \text{const}$) as the conditional line separating a rigid liquid from a soft fluid. If we choose as D the magnitude of the diffusion coefficient in the critical point, D_c, the line determined by the condition

$$D = D_c \quad (13)$$

will represent the dynamic continuation of the curve of the liquid–gas equilibrium. Note that the condition of constant viscosity, in contrast to the condition of constant diffusion, cannot be used as an approximation for the line of crossover $\tau^* \sim \tau_0$, since the viscosity not only is inversely proportional to the diffusion coefficient, but also is proportional to temperature and rapidly increases with compression along the line of constant diffusion. As a result, the lines of constant viscosity move with increasing temperature into the region of smaller densities, and at sufficiently high temperatures they even extend into the region of small (up to zero) pressures.

Naturally, the determination of the line of dynamic continuation of the boiling line based on condition (13) is only approximate. First, the condition $\tau^* \sim \tau_0$ corresponds to a sufficiently extended crossover, and the relation of the beginning of the line to the critical point is arbitrary. Second, we cannot neglect the change in the ratio a^2/τ_0 in the case of significant compression.

It is important to note that the dynamic line corresponds to a qualitative change in the temperature dependences of the diffusion coefficient and viscosity. Indeed, we have $\tau^* \sim \exp(E_{act}/k_B T)$ at low temperatures; consequently, $D \sim \exp(-E_{act}/k_B T)$. At the same time, at high temperatures $\tau^* \sim a/V_{th} \sim 1/T^{1/2}$, where V_{th} is the thermal velocity of particles, and for a rarefied gas $D \sim T^{1/2}$, while for a dense gas $D \sim T^{\alpha}$, where α is an index (close to 1/2) weakly changing with temperature [53]. Thus, the exponential temperature dependence of the diffusion coefficient near the dynamic line should be replaced by a power law. The viscosity at low temperatures also depends on temperature exponentially: $\eta \sim \exp(E_{act}/k_B T)$. This follows from both the Stokes–Einstein relationship $\eta \sim T/D$, and the Maxwell relationship $\eta = G_\infty \tau^*$, where G_∞ is the high-frequency limit of the shear modulus, whose value only weakly changes with temperature. At high temperatures, we have for the viscosity the relationship $\eta \sim T^{\beta}$, where β is a quantity close to 1/2. This follows both from the Stokes–Einstein relationship and from the Maxwell relationship with allowance made for the fact that $G_\infty \sim T$ in the high-temperature limit [54]. Consequently, the exponential decrease in the viscosity should be replaced near the dynamic line by a power-law dependence with increasing temperature.

Notice in conclusion of this section that a similar behavior should be characteristic of the thermal conductivity: the decrease in the thermal conductivity with increasing temperature in a rigid liquid should be replaced by its increase upon further heating in the range of the soft fluid.

4.4 Sound velocity and the thermal velocity of particles

At $P \sim 10^2 P_c$, the density reaches solid-like values, $\rho \sim 3\rho_c$, in the line of the constant magnitude of the diffusion coefficient. The change of τ_0 upon further compression can be estimated in terms of the Grüneisen model, according to which the Debye frequency increases with increasing density as $\omega_0 \sim \rho^{\gamma}$, where γ is the Grüneisen constant [55]. In the case of liquids, one can introduce the Grüneisen pseudoconstant [55]. For solids, the typical values are $\gamma \sim 1-3$. For such fluids as molecular liquids and liquid rare gases, $\gamma \sim 2-2.5$ [55, 56]. Taking into account that $a^2 \sim \rho^{-2/3}$, a weak increase in the diffusion coefficient should be observed in the dynamic line for these liquids at very high pressures with increasing pressure and density:

$$D \sim \rho^{1.3-1.8}.$$

Since the values of the Grüneisen pseudoconstant at superhigh pressures are unknown for most melts, we estimate the change in τ_0 upon compression in another way. To this end, we consider the qualitative difference in the character of particle motion in a liquid and in a quasigas fluid. In a liquid with a solid-like spectrum of vibrations, in the Debye approximation we have $\omega_0 = 2\pi/\tau_0 = V_s k_0$, where V_s is the sound velocity in liquid, and k_0 is the maximum value of the effective wave vector ($k_0 = \pi/a$). Consequently, $\tau_0 = 2\pi/\omega_0 = 2a/V_s$. On the other hand, in the ballistic regime of motion in the high-temperature limit the displacement of a particle by a distance a in fact corresponds to a single jump and occurs in a time $\tau^* = a/V_{th}$, where V_{th} is the thermal velocity of particles. Thus, condition (9) for the crossover from the vibrational to ballistic regimes can be written as $2a/V_s \sim a/V_{th}$, or

$$V_s \sim 2V_{th}. \quad (14)$$

The requirement that the thermal velocity of particles achieve half the velocity of sound in a condensed medium as a condition for the change in the regime of particle motion is quite reasonable from the physical point of view. The numerical factor 2 arises due to the fact that for most shortwavelength excitations the neighboring particles move

in antiphase, and their relative thermal velocity is equal to the sound velocity. In the gas phase, these two velocities are not independent, since the propagation of sound is by itself determined by the thermal motion of particles and depends only on temperature: $V_{\rm th} = (3k_{\rm B}T/m)^{1/2}$ and $V_{\rm s} = (vk_{\rm B}T/m)^{1/2}$, where v is the index of the gas adiabat ($v = 5/3$ for a monatomic gas, and $v = 7/5$ for a diatomic gas), and m is the mass of the particles. At the same time, the propagation of sound in a dense fluid is mainly determined by the interaction between the particles, whereas the sound velocity is determined by the high-frequency compression and shear moduli of the fluid and its density. Along the isochores, the moduli, as a rule, change insignificantly [34]; consequently, the sound velocities in the isochores also only weakly depend on temperature. At the same time, the thermal velocity of a classical particle decreases to zero with decreasing temperature, whereas at high temperatures it increases unrestrictedly. As a result, for each liquid at any density there is a temperature range in which the sound velocity and the thermal velocity of particles become comparable. The achievement of condition (14) with increasing temperature means that the particle stops 'feeling' the elasticity of the medium, similar to how the elasticity of the medium is not 'felt' by macroscopic objects that collide with relative supersonic velocities.

It should be noted that since the moduli of a substance are primarily determined by the potential energy of the particle interaction, condition (14), in fact, means that the kinetic and potential energies of particles in a condensed medium are comparable [see condition (11)]. At the same time, the proportionality coefficient in condition (11) can differ substantially from unity. Indeed, the barrier height for a particle jump is determined by elastic moduli, which, in turn, are second derivatives of the interaction energy with respect to volume, i.e., not only the absolute magnitude of the potential energy is of importance, but also the character of interparticle interaction. This was first noted by S M Stishov in paper [57], where it was shown that the potential energy of interaction $E_{\rm pot}$ for a van der Waals fluid near the critical point is close in magnitude to $k_{\rm B}T$, whereas for a Coulomb plasma with a compensating background in the form of a degenerate electron gas the following relationship is fulfilled near the critical point: $E_{\rm pot} \sim 3k_{\rm B}T$.

It should be also emphasized that conditions (9) and (14) are almost equivalent only at solid-like densities of the liquid, where the Debye approximation for the sound velocity is fulfilled. As a result, the condition $V_{\rm s} \sim 2V_{\rm th}$ will correspond to the change in the diffusion regimes for pressures $P > 10^2 P_{\rm c}$. Thus, the dynamic line of the crossover at low pressures corresponds to the line of almost constant diffusion and, beginning with some sufficiently high pressures, to the condition of the closeness of the values of sound velocity and doubled particle's thermal velocity.

4.5 Thermal energy and heat capacity

Although the zone of the change in the diffusion regime has a 'dynamic' nature, the thermodynamic functions also have specific features in the vicinity of the line of changing the diffusion mechanisms. This is related to the disappearance of transverse-phonon excitations for $\tau^* < \tau_0$. At temperatures close to the melting point, the solid-like nature of the spectrum of excitations in liquids at all frequencies ($2\pi/\tau^* < \omega \ll \omega_0$) has the effect that the heat capacity of the melt becomes close to that of the corresponding crystal, $c_V \sim 3k_{\rm B}$ (per particle) [34, 58]. With increasing temperature and with a corresponding decrease in τ^*, the contribution to heat capacity from transverse excitations decreases and the heat capacity becomes $2k_{\rm B}$ after the complete disappearance of transverse-phonon type excitations in the shortwavelength part of the spectrum [58]. At high density of the liquid, the contribution from the longitudinal excitations may be thought of as only weakly changing with increasing temperature up to values corresponding to the condition $\tau^* \sim \tau_0$. In this case, the thermal energy of the liquid, according to paper [58], is given by the expression

$$\frac{E}{N} = k_{\rm B}T\left[3 - \left(\frac{\tau_0}{\tau}\right)^3\right]. \tag{15}$$

A further increase in temperature and the corresponding decrease in the density lead to a transition from a dense fluid to an almost ideal gas, to a decrease in the contribution caused by longitudinal excitations, and to a further decrease in the heat capacity (per particle) to 'gas-like' values of $c_V \sim (3/2)\,k_{\rm B}$.

Certainly, such an approach is approximate, and the conception of longitudinal-phonon type excitations is by no means completely correct in the vicinity of the temperatures of the crossover in the diffusion regime. Nevertheless, the following estimate

$$c_V \sim 2k_{\rm B} \tag{16}$$

for the 'dynamic' line seems to be quite reasonable. At low pressures, the condition $c_V(T) = 2k_{\rm B}$ does not completely correspond to dynamic crossover because of the effect of near-critical anomalies on the heat capacity. The temperature of the disappearance of transverse excitations is related to a certain change in the temperature dependence of $c_V(T)$. The resolving of the excitations in liquid into transverse and longitudinal vibrations and jumps is rather arbitrary and, from the thermodynamic point of view, the transition will be merely smeared.

4.6 Dynamic line: computer simulation and experimental data

It was shown in Sections 4.1–4.5 that, on the basis of principal criterion (9), expressions (11), (13), (14), and (16) can be obtained for estimating the position of the dynamic line partitioning a liquid into two zones with different types of particle trajectories. For illustration, we performed computer molecular-dynamics calculations (see Appendix) and constructed lines determined by conditions (9), (11), (13), (14), and (16) for the fluids of real substances (Ar, Ne, and N_2) based on the data of NIST compilation [34] and for model systems of particles with a Lennard-Jones potential and soft-sphere potential $U(r) = Ar^{-n}$ with different exponents n in the repulsion potential (see also Refs [40, 41]). Recall that the Lennard-Jones potential rather well reproduces the behavior of many molecular substances and rare gases, whereas the soft-sphere potential describes the behavior of the substance in the superhigh-pressure limit, when the attractive part of the interaction potential can be neglected. In calculations, we used conditions of the exact equality for all the criteria: $\tau^* = \tau_0$, $3k_{\rm B}T/2 = E_{\rm pot}$, $D = D_{\rm c}$, $V_{\rm s} = 2V_{\rm th}$, and $c_V = 2k_{\rm B}$. The magnitude of τ_0 was estimated both from an analysis of particle trajectories and from the correlation functions of particle motion.

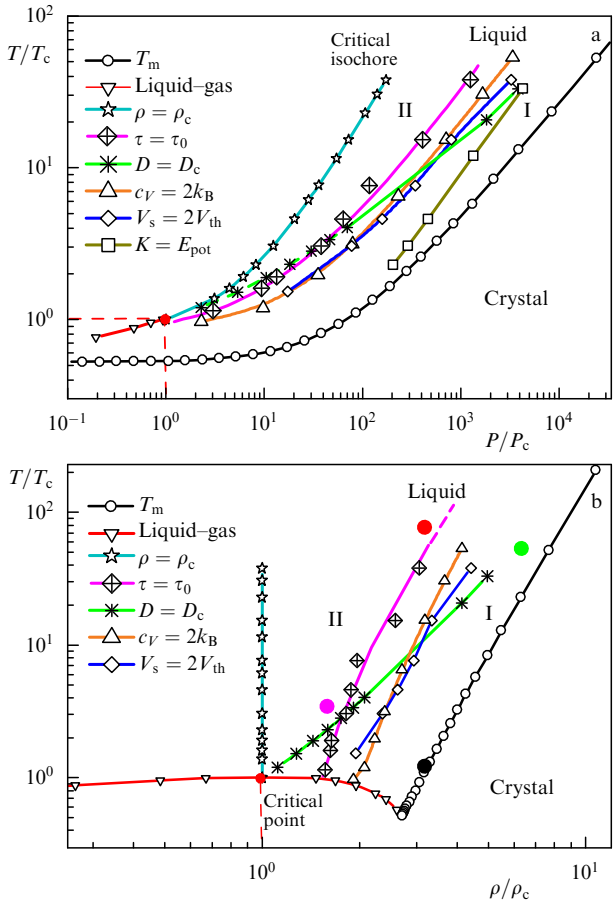

Figure 11. (a) $P-T$, and (b) $\rho-T$ phase diagrams for a system of particles with the Lennard-Jones potential (calculated lines corresponding to various criteria are shown; see the main text). Region I is appropriate to liquid, and region II corresponds to quasigas fluid. Black circles in figure (b) mark the parameters at which the trajectories shown in Fig. 9 were simulated.

The positions of all lines in the $P-T$ and $\rho-T$ phase diagrams are shown in Figs 11–14. Good agreement is seen between the lines constructed on the basis of different criteria. That the difference between the temperatures in different lines is equal to several dozen percent should not be surprising, since the coefficients of proportionality in Eqns (9), (13), (14), and (16) and especially in Eqn (11) can substantially differ from unity. Thus, in the dynamic line we have $3k_BT/2 \approx 5E_{pot}$ for a system of particles with a Lennard-Jones potential. At low pressures ($P < 10P_c$), the lines determined by conditions (14) and (16) slightly deviate from the main line (9) due to the effect of hypercritical anomalies and the invalidity of the Debye approximation at low densities of the fluid. In addition, for a system of soft spheres with $n = 12$, points of calculated minima of viscosity are shown, which are almost coincident with the position of the dynamic line.

Good agreement between experimental data for fluids of real substances and calculated values for a system of particles interacting via a Lennard-Jones potential is evidenced (see Fig. 12). Recently, the method of inelastic X-ray scattering was used to study the dynamics of excitations in liquid argon and nitrogen at various pressures and temperatures [35, 48]. It turned out that a qualitative change is observed in the spectrum of excitations at certain parameters; namely, a positive dispersion of acoustic excitations is observed at higher pressures, i.e., an increase in the sound velocity with

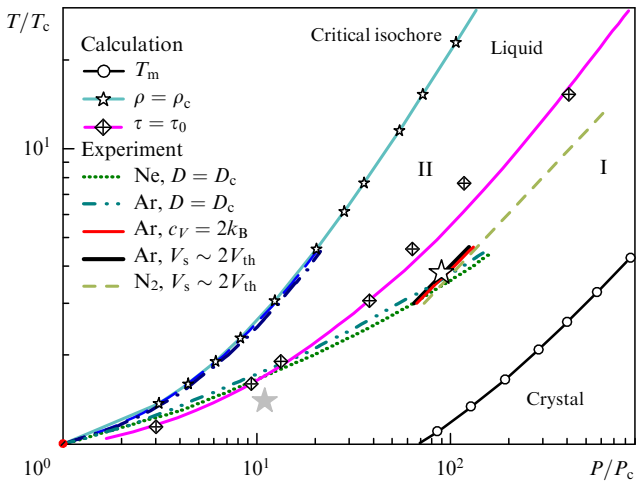

Figure 12. $P-T$ phase diagram for a system of Lennard-Jones particles (for designations, see Fig. 11). The calculated curve meeting the criterion $\tau = \tau_0$ is compared with the experimental dependences for Ne, Ar, and N_2 [34]. The star symbols mark the experimental parameters (open star for Ar [35], and gray star for N_2 [48]) at which the positive dispersion of acoustic excitations in liquids disappears. Experimental critical isochores [34] for Ne and Ar are also given.

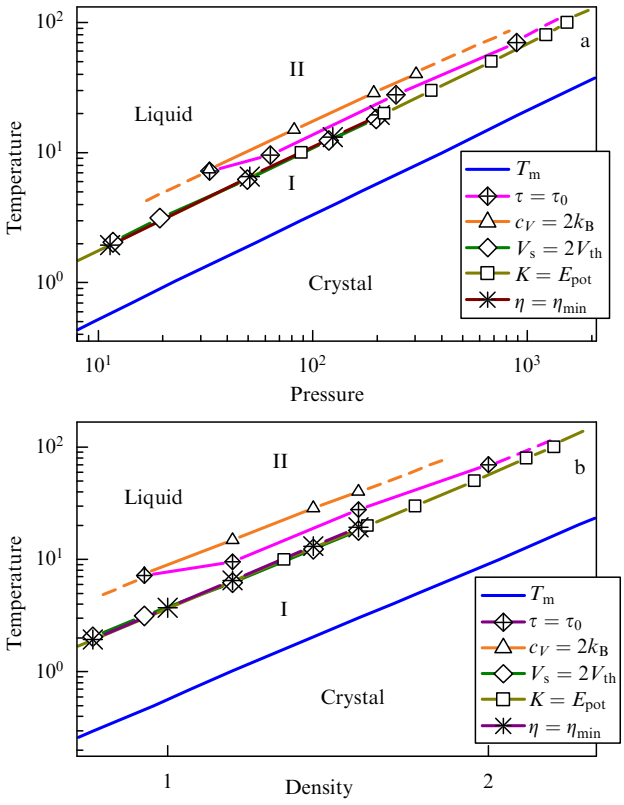

Figure 13. (a) $P-T$, and (b) $\rho-T$ phase diagrams for a system of soft spheres with an exponent $n = 12$ in the interaction potential. Calculated dependences meeting various criteria are shown.

decreasing wavelength, whereas at lower pressures no positive dispersion manifests itself. The authors of Ref. [35] ascribed (erroneously, in our opinion) the point of the change in the type of the excitation spectra to the extension of the Widom line. It is obvious that the regions of loss of fast sound for argon [35] and nitrogen [48] fluids are located near the calculated dynamic lines (see Fig. 12).

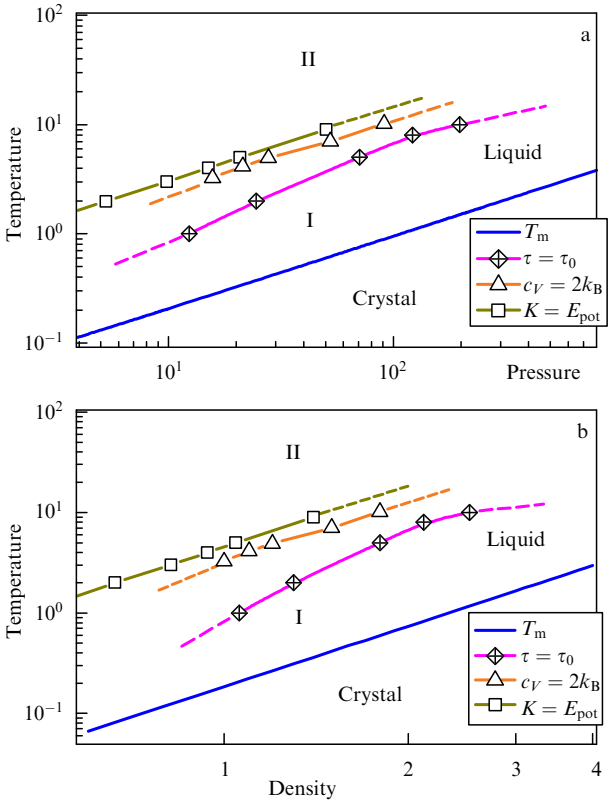

Figure 14. (a) $P-T$, and (b) $\rho-T$ phase diagrams for a system of soft spheres with an exponent $n = 6$. Calculated dependences meeting various criteria are demonstrated.

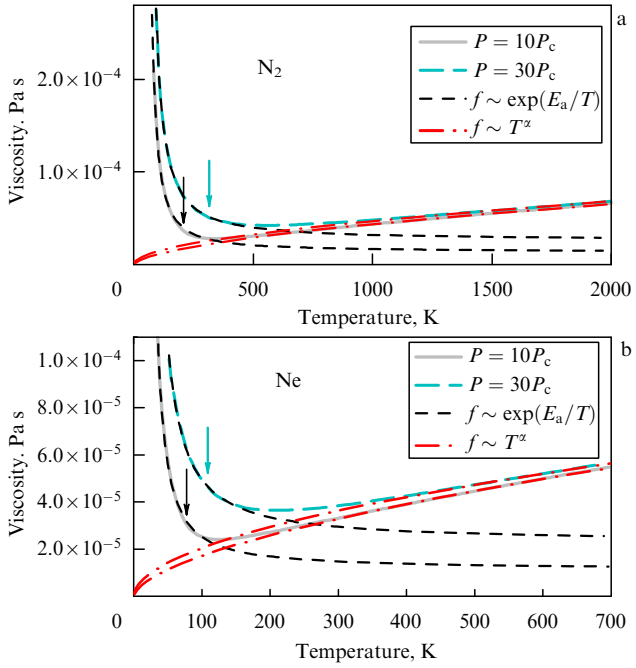

Figure 15. Experimental isobaric temperature dependences of the viscosity [34] for (a) nitrogen, and (b) neon with asymptotics at low temperatures (activation exponent) and high temperatures (power function). The arrows indicate the temperatures meeting the dynamic criterion $\tau = \tau_0$. The exponents α are equal to 0.596 at $P = 10P_c$, and 0.528 at $P = 30P_c$ for N_2 and, correspondingly, 0.593 and 0.517 for Ne.

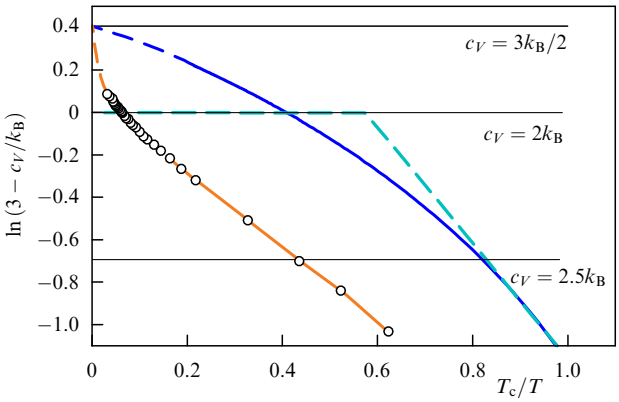

Figure 16. Dependences of the specific heat reduced to the quantity $\ln(3 - c_V/k_B)$ on the reciprocal temperature for a Lennard-Jones liquid (circles with the interpolation curve) in the isochore (calculated at $\rho = 1$), (solid line) for argon in the isobar ($P = 50P_c$), and (dashed lines) according to a simplified model [58]. The dashed extensions of the first two dependences show their extrapolations to the state of an ideal gas.

For a system of soft spheres, the positions of all lines determined applying different criteria agree well with each other (see Figs 13, 14). Thus, the dynamic line of the change in the type of particle trajectories, in contrast to the Widom line, is not related to the existence of the boiling line and critical point. Consequently, the dynamic line of the change in the type of particle trajectories and diffusion regime will also take place in those macromolecular and colloid systems in which the liquid–gas transition is completely absent [59–61].

Figure 15 displays the temperature dependences of the viscosity of liquid Ne and N_2 at various pressures. It is seen that the regions of the change in the type of dependences in which the exponential descending dependence is replaced by an increasing power-law dependence correspond in temperature to the position of the dynamic line.

Figure 16 depicts the experimental and calculated dependences of the heat capacity c_V along the isobar and isochore. The heat capacity decreases smoothly from $3k_B$ to $(3/2)\,k_B$ (per particle), and the dynamic line approximately satisfies the condition (16): $c_V = 2k_B$. The figure also demonstrates the behavior of the heat capacity in terms of the simplified model [58] [see Eqn (15)], according to which the main contribution to the decrease in the heat capacity comes from the disappearance of transverse waves from the excitation spectrum.

4.7 Dynamic line and melting line in the phase diagram

It should be emphasized that dynamic lines, in contrast to the Widom line, are appropriate to an increase in density (see Figs 11–14). At superhigh pressures, the following relationship is valid for the lines of dynamic crossover: $\rho \sim T^k$, where $k \sim 0.2-0.3$. This relationship between the density and temperature is fulfilled to a good accuracy along the lines of the change in the diffusion mechanisms both for real molecular substances and for model systems with a Lennard-Jones potential and the soft-sphere potential with $n = 12$ (see Figs 11–13).

It should be noted that the behavior of systems with a power-law pairwise potential, including a system of Lennard-Jones particles, becomes at superhigh pressures similar to the behavior of a system of soft spheres [62]. For the last system, as for any system of particles with a homogeneous potential, scaling relationships exist for all physical quantities along the lines in the phase diagram, where the similitude of phase trajectories is retained [63–66]. For thermodynamic proper-

ties that are determined by the nonideal part of the partition function, this follows from the Klein theorem [62–64]. Hoover et al. [65] suggested, based on qualitative considerations, that for a system of soft spheres certain scaling relationships should also be fulfilled for kinetic characteristics. Later on, this was more rigorously proved by Zhakhovskii [66]. For the melting curve of the system of soft spheres, the relationship $\rho \sim T_m^{3/n}$ is fulfilled [62]. At $n = 12$, we have $\rho \sim T_m^{1/4}$. For the pressure P and magnitudes of the B and G_∞ moduli along the melting curve of the system of soft spheres at $n = 12$, an identical functional dependence (P, B, $G_\infty \sim T_m^{5/4}$) is observed, while the dependence $D \sim T_m^{5/12} \sim \rho^{5/3}$ can be seen for the diffusion coefficient [65, 66]. Notice that the lines of constant diffusion converge with the melting curve for the system of soft spheres, since the diffusion coefficient increases unrestrictedly along the melting curve [66]. For Lennard-Jones particles, the $D = D_c$ line joins with the melting curve at $P \sim 10^4 P_c$ and $\rho \sim 10\rho_c$ (see Fig. 11).

It can be noted that the functional dependences $\rho(T)$ and $D(\rho)$ for the melting curve of the system of soft spheres and for the dynamic line of the change in the mechanism of diffusion are rather close, which appears to be not by mere chance. The type of phase trajectories in the line of the change in the character of diffusion for the system of soft spheres is also retained upon scaling the velocities and coordinates of particles, just as in the melting curve. Thus, the same functional relationships are fulfilled in the line of crossover of the mechanism of diffusion for soft spheres, as in the case of the melting curve. This is also the case for Lennard-Jones particles at superhigh pressures. It can be concluded that the dynamic line of the change in the diffusion mechanism for the system of particles with an m/n potential at high pressures runs similar to the melting curve, i.e., the zone of 'true' liquid and the very dynamic line do not disappear at any pressures.

The smaller the exponent n in the repulsion potential of soft spheres, the wider the region of the low-temperature solid-like liquid (see Figs 13, 14). For the pressure dependence of the temperature of the dynamic line, the following relationship is approximately fulfilled: $T_d(P) \approx (60/n)\, T_m(P)$. For the Lennard-Jones system and the system of soft spheres with $n = 12$, the temperature of the dynamic line in isobars is approximately five times greater than the melting temperature (see Figs 11, 13). For metals, in view of their softer repulsion potential at superhigh pressures, this ratio is even greater. In contrast, as the exponent increases in the repulsion potential, the region of solid-like liquid narrows, and for $n > 60$ the crystal formed by soft spheres melts directly into a quasigas fluid. In particular, condition (16), $c_V \sim 2k_B$, is fulfilled near the melting curve at $n \sim 60$. For $n > 60$, the dynamic line lies below the melting curve and establishes a line of demarcation between the low-temperature harmonic state of the crystal with well-defined transverse acoustic phonons and the high-temperature hard-sphere-crystal anharmonic state, in which the particles move mainly ballistically outside the domain of the action of the interaction potential. Condition (9), $\tau^* \sim \tau_0$, in this case means that the particle in the crystal moves almost harmonically and ballistically for comparable time periods.

For a system of hard spheres, which is the limiting case of a system of soft spheres, the absence of the solid-like liquid with transverse phonon excitations is obvious. For hard spheres, the potential energy of interaction is zero, namely $c_V = (3/2)\, k_B$ at all temperatures, and the harmonic vibrations in the crystal of hard spheres are absent.

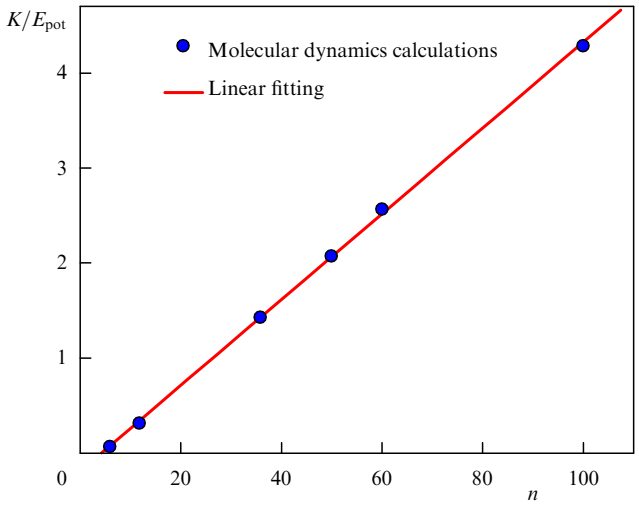

Figure 17. Ratio of the kinetic energy to the potential energy for a soft-sphere liquid near the melting curve (this quantity virtually does not change along the curve) as a function of the exponent n in the interaction potential.

The ratio of the kinetic energy of particles to the potential energy of their interaction in the melting lines of soft spheres varies from zero for the system with $n = 3$ to infinity as $n \to \infty$ (hard spheres) (Fig. 17).

It is well known that the liquid–gas curve in the phase diagram is absent for a system of particles with a large repulsion exponent and small region of attraction; instead, there is a line of an isostructural transition with a critical point in the crystalline state [59, 60]. The dynamic line in such systems apparently will separate states of the crystal with different types of excitations in the hypercritical region of a given isostructural transition. Consequently, in many macromolecular and colloidal systems, in which the liquid–gas transition is totally absent, the dynamic line will lie in the region of stability of the solid phase and separate the harmonic and anharmonic states of the crystal.

The systems of particles with a soft-sphere interaction potential have been actively studied in several hundred papers. However, the fact concerning the existence of critical values in the region of large n, at which qualitative changes in the behavior of the system occur, had not been realized earlier. The kinetic and potential energies in the melting curve become comparable at $n \approx 27$, and condition (16) is fulfilled at $n \approx 60$. Thus, the melts of systems of soft spheres with $n \sim 10$ and with $n \sim 100$ near the melting line feature qualitative differences: high-frequency transverse excitations can propagate in the first melt, whereas they do not propagate in the second one. Correspondingly, the diffusion process in a liquid of soft spheres proceeds for $n > 60$ via a large number of small ballistic type jumps, and no vibrations of particles near the equilibrium positions are observed in such liquids. Earlier work on computer simulation of diffusion in the hard-sphere liquid did not indeed reveal the vibrational-hopping mechanism, which for a long time even served as an argument against the possibility of the existence of the hopping mechanism of diffusion in liquids entirely [67]. In reality, diffusion in a hard-sphere liquid and in a soft-sphere liquid for $n \ll 60$ (e.g., at $n = 12$) near the melting temperature is of a qualitatively different character.

These results are very important for the understanding of differences in the vitrification phenomena in liquids and of geometrical jamming in the systems of hard and soft spheres with increasing density. The problem of the similarity and difference between these phenomena has been actively discussed in recent years [68, 69]. At very large n ($n > 100-150$), the liquid–glass transition in a supercooled melt occurs in the state of soft quasigas fluid, just as the glass transition in a hard-sphere liquid, and is determined by the conditions of geometrical confinement (jamming). Thus, vitrification in the systems of soft spheres for $n \ll 100$ and of almost hard spheres with $n > 100$ is of a qualitatively different character. It is obvious that the temperature dependences of the viscosity and diffusion coefficients near the glass transition temperature in these two cases should differ qualitatively.

It should be noted that the dynamic line under consideration lies at very high temperatures ($\sim 10^4$ K) and pressures (10 GPa) for metallic, ionic, and covalent melts; therefore, these experimental conditions are experimentally accessible only in shock-wave investigations. At the same time, the dynamic line for many molecular liquids and liquid rare gases lies in the range of high pressures that is accessible for experimental physics. Thus, it can be expected that the transition from a solid-like liquid to a quasigas-like fluid for neon at a pressure of 3 GPa should be observed at temperature $T \approx 1000$ K, which is approximately five times greater than the melting temperature. For many macromolecular and colloidal systems, the dynamic line also lies in the experimentally accessible range.

In conclusion, note once more that, earlier, attempts were undertaken to relate the qualitative changes in the excitation spectrum of supercritical fluids with the extrapolation of the Widom line [35]. It should be emphasized that, in reality, the Widom line and the dynamic line corresponding to the change in the diffusion mechanism have different natures. The Widom line represents several lines continuing the liquid–gas line, which adjoin the isochore from the side of the lowered density and end at $T \sim (2-2.5)\,T_c$ and $P \sim (10-15)\,P_c$. At the same time, the dynamic line corresponds to the increase in the density with increasing temperature and does not terminate in the region of superhigh pressures and temperatures ($P > 10^4 P_c$ and $T > 10^2 T_c$). Moreover, the dynamic line is not formally related to the liquid–gas transition; it can also exist for systems in which the boiling curve and the critical point are entirely absent.

4.8 Frenkel line

> *Frenkel was a theoretician physicist. By this, I wish to emphasize that he was primarily interested in what occurs in real objects, and the mathematical methods he employed served his physics rather than vice versa, in contrast to what sometimes happens with representatives of the modern generation of scientists. The validity of this statement follows, it can be said, from each page of his book about liquids. He asks: "What occurs in reality and how can this be explained?" — and asks himself this question precisely, rather than in a form like: "Here is an elegant theory. Does it work? If the experiment contradicts it, this appears to mean that the experiments are erroneous... ."*
>
> I E Tamm [70]

As was already said above, the concept of a liquid as a state of matter with a certain short-range order and a crystal-like spectrum of excitations at high frequencies became commonly accepted only at the end of the 20th century. However, as far back as the 1930s, Ya I Frenkel in the Soviet Union developed a kinetic theory of liquids precisely on the basis of the similarity of features of the liquid and solid states [11]. Many of Frenkel's views, e.g., concerning the hole structure of liquids or his mechanistic estimates of the activation energy for diffusion, are excessively simplified or erroneous from the standpoint of the modern theory of liquids. Nevertheless, most of the qualitative conclusions following from Frenkel's models proved to be true. It was precisely Frenkel who correctly introduced the concept of liquid relaxation time τ^* and gave a microscopic interpretation of Maxwell's relaxation time [42]. The differentiation of the types of particle motion in liquids into vibrations near positions of local equilibrium and jumps between these positions is, to a certain extent, arbitrary, especially at comparable values of τ^* and τ_0. Nevertheless, the results of computer simulation for the systems of particles with different types of interaction potentials show that such a differentiation is quite reasonable. Moreover, the introduction of the concept of a relaxation time makes it possible to circumvent the insolvable (in modern theoretical physics) problem of the calculation of energy barriers between various states in a system with a large number of interacting particles.

Frenkel showed that in liquids at high frequencies (higher than the inverse relaxation time) transverse shear waves should propagate. He noted in book [11] that the absence of the experimental observation of the propagation of shear waves in liquids appears to be related to the small magnitude of the relaxation time for most melts. Moreover, Frenkel showed that longitudinal waves in liquids should propagate in the entire frequency range, but the character of their propagation should change at frequencies on the order of the inverse relaxation time, i.e., he predicted the phenomenon of fast sound. For many viscous liquids, the existence of both transverse acoustic excitations and of positive dispersion of longitudinal waves was established experimentally several decades (!) later. When describing the increase of the relaxation time observed with decreasing temperature, Frenkel noted that the very process of glass transition indicates that the division of substances into solids and liquids is rather arbitrary; it is made from practical considerations and depends on the duration of the observation process. Thus, Frenkel, in fact, was a creator of the kinetic approach to the theory of glass transitions.

Nevertheless, Frenkel's work in this field did not receive proper appreciation from contemporaries. His treatment of liquids based on their similarity with solids rather than with gases was too unconventional, differing too much from traditional concepts which had been developed for centuries. Frenkel's monograph, *Kinetic Theory of Liquids* [11], in many ways was ahead of its time. Frenkel himself certainly realized that his theory was rough and approximate. In the preface to the first edition of the book, he noted that "the publication of a book devoted to the kinetic theory of liquids may seem to be untimely." At the same time, Frenkel believed that three circumstances lent justification: (1) he had dealt with these problems for more than 20 years and many results remained unpublished; (2) a very limited number of physicists had the right understanding of the principles of the kinetic theory of liquids, and (3) "a description of a new theory, even in a crude and incomplete form, will favor the attraction of attention of other scientists to this subject and the acceleration of its

further development.'' Nevertheless, the Frenkel theory even in the Soviet Union was mainly employed to describe the behavior of only viscous liquids in a state close to glass transition, i.e., it was implicitly supposed that there is a qualitative difference between liquids with high and low viscosities. In reality, the difference is only quantitative: for ultraviscous liquids in a state close to glass transition, the relaxation time is $\tau^* \sim 10^2$ s, whereas for the majority of molecular and metallic liquids close to the state of melting, one finds $\tau^* \sim 10^{-12}-10^{-11}$ s. In the middle of the 20th century, the most easily available sources of ultrasound were those with frequencies ranging $\sim 10^8-10^9$ Hz. Transverse vibrations at these frequencies propagate only in liquids with relaxation times $\tau^* > 10^{-9}-10^{-8}$ s and viscosities $\eta > 1-10$ Pa s. The employment of the methods of Brillouin scattering [5–7], inelastic neutron scattering, and recently also inelastic X-ray scattering [8, 9] made it possible to extend the investigations of the dynamics of liquids into the range of higher frequencies, up to the frequency of order 10^{13} Hz (the maximum feasible in condensed media). At these frequencies, the transverse acoustic waves can propagate in all liquids, including liquid metals, liquid rare gases, and molecular liquids. Thus, in the 70 years after Frenkel developed his model, it became clear conclusively that no qualitative difference exists in the dynamics of excitations of liquids such as silica melt and water or liquid gallium. Note, however, that to date in many textbooks for students there are statements that the transverse acoustic waves cannot propagate in liquids, in contrast to those in solids.

Ya I Frenkel's range of interests was very wide: it involved the electron theory of solids, the physics of the condensed state and the physics of the atomic nucleus, general problems of quantum mechanics and electrodynamics, astrophysics, and geophysics. In the majority of fields, he obtained notable results. His name was given to a whole number of physical objects and phenomena: the Frenkel exciton, Frenkel defects, the Bohr–Frenkel–Wheeler liquid-drop model of atomic nuclei, etc. Since Frenkel's work on the kinetic theory of liquids was underestimated in due time, we suggest that the line determined by the condition $\tau^* \sim \tau_0$ be called the *Frenkel line*. The thus-defined Frenkel line separates a rigid liquid with a solid-like spectrum of excitations at high frequencies and hopping mechanism of diffusion (it is just such a liquid that was considered by Frenkel) from a soft (quasigas) fluid, in which the spectrum does not contain transverse acoustic excitations and the diffusion is dominated by particle collisions. Thus, any liquid in the hypercritical region can exist in two qualitatively different states — low-temperature and high-temperature — and the Frenkel line represents a boundary between these states.

5. Conclusions

As discussed above, the thermodynamic continuation of the boiling curve into the hypercritical region (Widom line) and the line of the change in the type of dynamics of particle motion (Frenkel line) lead to qualitatively different results (Fig. 18). The Widom line, in fact, represents a wide bunch of lines continuing the boiling line, which adjoin the isochore on the side of lower densities, and ending at $T \sim (2-2.5)\,T_c$ and $P \sim (10-15)\,P_c$. In contrast, the Frenkel line represents a narrow band which is not formally restricted in pressure or temperature. This line exists even in systems in which the boiling curve and critical point are wholly absent. It is

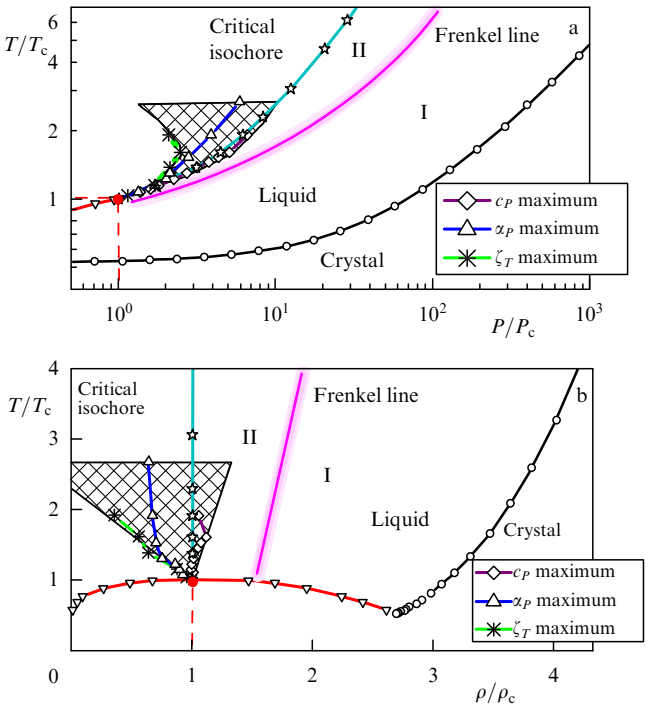

Figure 18. (a) $P-T$, and (b) $\rho-T$ phase diagrams for the systems of particles with a Lennard-Jones potential. Positions of the beginning of the Frenkel line (criterion $\tau \sim \tau_0$) and of the Widom region (hatched region), which is determined by the lines of maxima of c_P, α_P, and ζ_T, are compared (see Fig. 5: the main designations of the lines are the same). Region I corresponds to a liquid, and region II corresponds to a quasigas fluid.

precisely this line that is constructively suited for the role of the boundary between a liquid and a quasigas type supercritical fluid. In many macromolecular and colloidal systems, where no liquid–gas transition is observed at all, the dynamic line can lie not only in the region of liquid stability, but also in the region of stability of the solid phase and separate harmonic and anharmonic states of crystal.

First-principles theories of the liquid state that 'start' from a dense gas describe the soft fluid above the Frenkel line, whereas most of the experimental data have been obtained for the low-temperature 'rigid' state of liquids. At pressures $P < (10-10^2)\,P_c$, the condition of the constant magnitude of the diffusion coefficient, $D = D_c$, where D_c is the value of the diffusion coefficient near the critical point, can be used for the estimation of the position of the Frenkel line. For $P > 10P_c$, the condition of the equality of the sound velocity to the doubled thermal velocity of particles and the condition of a decrease in the heat capacity of the liquid to a magnitude of $c_V \sim 2k_B$ (per particle) can also be used for the same purpose. Note that the sound velocity can easily be measured in shock-wave investigations at pressures up to a megabar range. As an experimental criterion of the intersection of the Frenkel line, the observation of the disappearance of positive dispersion of acoustic waves in liquids can also be used at present. In the future, with a further development of the methods of inelastic X-ray scattering, the direct observation of the loss of transverse acoustic excitations in liquids upon reaching the Frenkel line will be possible as well.

Acknowledgments. We are grateful to S M Stishov, H F Stanley, P McMillan, G Simeoni, and F A Gorelli for fruitful discussions of our work and helpful remarks. This

work was supported in part by the Russian Foundation for Basic Research (project Nos 11-02-00303, 11-02-00341, 10-02-01407), by Programs of the Presidium of the Russian Academy of Sciences, and by the RF Ministry of Education and Science projects 8370 and 8512. One of us (K T) was also supported by the UK Engineering and Physical Sciences Research Council (EPSRC) Foundation.

6. Appendix: Calculation methods

Most of the calculation details are highlighted in the original papers, including our work [31, 32, 40, 41]. Some calculations were performed specially for this review. For convenience, it is reasonable to briefly describe the main aspects of the calculations.

To illustrate properties of the liquid and gas phases for the Lennard-Jones system, we used both literature data [71–73] and computer simulation by the molecular-dynamics method. In the literature there is a wide spectrum of data concerning this system. One of the most complete investigations into the Lennard-Jones system was performed in Meier's dissertation [72], where such data as the equation of state, internal energy, heat capacity at constant volume, diffusion constant, and shear and bulk viscosities, were presented for the Lennard-Jones system at more than a hundred points of P and T. Thus, a large database was accumulated for this system. We used the results of Ref. [72] for studying various properties of the system at low temperatures. Based on the interpolation of the data on the equations of state and energy, values of the isothermal compressibility $\beta = (1/\rho)/(\partial\rho/\partial P)_T$, thermal expansion $\alpha = -(1/\rho)/(\partial\rho/\partial T)_P$, and thermal fluctuations $\langle\Delta N^2\rangle/N^2 = (\partial\rho/\partial P)_T$ have been obtained. The heat capacity at constant pressure was calculated by differentiating enthalpy along the isobars.

To separate the quasigas and liquid mechanisms of particle motion far from the critical point, the thermodynamic and dynamic properties of the system at high densities and temperatures should be known. Such data were absent in the available literature. Therefore, we performed computer simulation of the properties of the Lennard-Jones system along the melting curve and in the vicinity of this curve on the liquid side [31, 40, 41].

The melting curve of the Lennard-Jones system was calculated, at high temperatures as well, in Ref. [73]. In our work, we calculated the diffusion coefficient, shear viscosity, elasticity modulus at the infinite frequency, and the liquid relaxation time along the melting curve at temperatures of up to $T = 100.0$ in reduced Lennard-Jones units [40, 41]. In addition, we calculated the thermodynamic and transport properties of the system along some isochores ($\rho = 0.85$, 1.0, 1.15, 1.3, 1.56) and isotherms ($T = 10.0$, 20.0, 30.0, 50.0); this permitted us to accumulate data for high densities and temperatures, which, together with available literature data, were used for an analysis of the behavior of the system. The equations of motion were integrated using the velocity form of the Verlet algorithm. Depending on the density, the number of particles in our simulation was varied from $N = 1000$ to $N = 4000$. The cutoff radius of the interaction potential was chosen to be $r_c = 2.5\sigma$. Let us recall that the cutoff radius does not affect the dynamic properties of the system. In our simulation, the system was thermalized for 5×10^5 steps; after this, we calculated the properties of interest over an interval of 3×10^6 steps. The time step was chosen to be $dt = 0.001$ (in Lennard-Jones units). The diffusion coefficient was calculated using the Einstein formula, and the viscosity was calculated via the Kubo formula.

The position of the critical point for the Lennard-Jones system has been widely discussed in the literature. However, to date there are some discrepancies in the determination of the critical parameters. In this review, we used the following values of the critical temperature, density, and pressure (in Lennard-Jones units): $T_c = 1.31$, $\rho_c = 0.314$, and $P_c = 0.129$. The kinetic energy per particle is $K/N = 3k_BT/2$, and the potential energy corresponds to the total interaction energy. In the case of the pairwise potential, a complicating circumstance is the change in the sign of the potential energy; for the Lennard-Jones system, the potential energy was taken in the form $E_{pot} = E_{LJ}(V) - E_{LJ}(V_0) + P_0(V_0 - V)$, where the V_0 value corresponded to the volume at a maximum possible negative pressure P_0 at the zero temperature. The high-frequency limit of the shear modulus of the liquid, G_∞, was calculated via formulas suggested in Ref. [54]. The compressibility modulus was determined using the equation of state as $B = \beta^{-1} = \rho(\partial\rho/\partial P)_T$.

The diffusion coefficients for real substances were calculated from the Stokes–Einstein relationship $D \sim T/\eta r_0$, where r_0 is the effective size of the particle, using the experimentally determined values of the viscosity [34]. The lines of the constant ratio of the particle velocities for real substances (argon and nitrogen) were obtained from the experimental sound velocities and calculated thermal velocities $v_{th} = (3k_BT/m)^{1/2}$. Upon simulation, the velocities of longitudinal and transverse components of sound were calculated from the data on the density and on the compression and shear moduli: $v_s \sim (B/\rho)^{1/2}$, and $v_{st} \sim (G_\infty/\rho)^{1/2}$, respectively. The magnitude of τ_0 was estimated from an analysis of both trajectories of atom motion (see Fig. 9) and autocorrelation functions of particle motion (see Fig. 10). The relaxation time τ in the liquid was determined as the average time of particle displacement by an interatomic distance. Correspondingly, this time can be estimated from the diffusion coefficient as $\tau = \rho^{-2/3}/(6D)$. Note that τ_0 can be estimated reliably only at sufficiently low temperatures, where the vibrational mechanism in liquids is well determined, whereas τ can be calculated from the diffusion coefficients at all temperatures. We calculated τ_0 and τ along the isochores and extrapolated the temperature dependences up to their intersection. The accuracy of determining the temperature of the dynamic crossover, $\tau = \tau_0$, is $\pm(20-30)\%$; the error in the calculations of other quantities is less than 10%.

Notice that the liquid relaxation time is frequently determined from the expression $\tau^* \sim \eta/G_\infty$, which 'works' well in the case of high-viscosity liquids. However, for a fluid with a low viscosity, this expression formally gives very small values of τ^*. The reason is that in the case of such a definition the relaxation time corresponds to the shortest time of the change in the local configuration existing around the particle, and no particle's jump occurs in this time. The expressions $\tau^* \sim a^2/D$ and $\tau^* \sim \eta/G_\infty$ coincide (with allowance for the Stokes–Einstein relationship) at $G_\infty = \rho T$. The quantity ρT (which is, in fact, the ideal-gas pressure) for fluids is frequently considered as the translational part of the total quantity G_∞.

In the line of the change in the dynamic mechanism, a qualitative change occurs in the trajectories of particle motion (see Fig. 9). The magnitude of τ^*, just as of τ_0, can be estimated directly from an analysis of trajectories of atomic

motion (see Fig. 9); in this case, good agreement with the estimate $\tau^* \sim a^2/D$ is obtained. The constant values of the ratio of sound velocities for real fluids were determined by 'sewing' lines $D = D_c$, $v_s/v_{th} = \text{const}$, and $v_{st}/v_{th} = \text{const}$ at $P \sim 10^2 P_c$. The average value of the constants proved to be 2.2. The experimental data for $c_V(T, P)$, $c_P(T, P)$, $\rho(T, P)$, etc. for Ar, Ne, and N_2 were taken from the database of the National Institute of Standards and Technology (NIST) [34].

References

1. Kiran E, Debenedetti P G, Peters C J (Eds) *Supercritical Fluids: Fundamentals and Applications* (Dordrecht: Kluwer Acad. Publ., 2000)
2. Likal'ter A A *Usp. Fiz. Nauk* **170** 831 (2000) [*Phys. Usp.* **43** 777 (2000)]
3. Supercritical fluid, http://en.wikipedia.org/wiki/Supercritical_fluid
4. Hansen J P, McDonald I R *Theory of Simple Liquids* (London: Academic Press, 1986)
5. Grimsditch M, Bhadra R, Torell L M *Phys. Rev. Lett.* **62** 2616 (1989)
6. Pezeril T, Klieber C, Andrieu S, Nelson K A *Phys. Rev. Lett.* **102** 107402 (2009)
7. Jeong Y H, Nagel S R, Bhattacharya S *Phys. Rev. A* **34** 602 (1986)
8. Hosokawa S et al. *Phys. Rev. Lett.* **102** 105502 (2009)
9. Giordano V M, Monaco G *Phys. Rev. B* **84** 052201 (2011)
10. Scopigno T, Ruocco G, Sette F *Rev. Mod. Phys.* **77** 881 (2005)
11. Frenkel J *Kineticheskaya Teoriya Zhidkostei* (Kinetic Theory of Liquids) (Moscow–Leningrad: Nauka, 1975) [Translated into English (Oxford: The Clarendon Press, 1946)]
12. Wallace D C *Phys. Rev. E* **56** 4179 (1997)
13. Chisolm E D, Wallace D C *J. Phys. Condens. Matter* **13** R739 (2001)
14. Brazhkin V V, Buldyrev S V, Ryzhov V N, Stanley H E (Eds) *New Kinds of Phase Transitions: Transformations in Disordered Substances* (Dordrecht: Kluwer Acad. Publ., 2002)
15. Roberts C J, Panagiotopoulos A Z, Debenedetti P G *Phys. Rev. Lett.* **77** 4386 (1996)
16. Gorelli F et al. *Phys. Rev. Lett.* **97** 245702 (2006)
17. Santoro M, Gorelli F A *Phys. Rev. B* **77** 212103 (2008)
18. Katayama Y et al. *Nature* **403** 170 (2000)
19. Monaco G et al. *Phys. Rev. Lett.* **90** 255701 (2003)
20. Stanley H E *Introduction to Phase Transitions and Critical Phenomena* (New York: Oxford University Press, 1971) [Translated into Russian (Moscow: Mir, 1973)]
21. Xu L et al. *Proc. Natl. Acad. Sci. USA* **102** 16558 (2005)
22. Nishikawa K et al. *J. Chem. Phys.* **118** 1341 (2003)
23. Nishikawa K, Morita T *Chem. Phys. Lett.* **316** 238 (2000)
24. Sato T et al. *Phys. Rev. E* **78** 051503 (2008)
25. Fisher M E, Widom B *J. Chem. Phys.* **50** 3756 (1969)
26. Widom B, Rowlinson J S *J. Chem. Phys.* **52** 1670 (1970)
27. Franzese G, Stanley H E *J. Phys. Condens. Matter* **19** 205126 (2007)
28. Artemenko S, Lozovsky T, Mazur V *J. Phys. Condens. Matter* **20** 244119 (2008)
29. Kumar P, Franzese G, Stanley H E *Phys. Rev. Lett.* **100** 105701 (2008)
30. Kumar P, Franzese G, Stanley H E *J. Phys. Condens. Matter* **20** 244114 (2008)
31. Brazhkin V V et al. *J. Phys. Chem. B* **115** 14112 (2011)
32. Brazhkin V V, Ryzhov V N *J. Chem. Phys.* **135** 084503 (2011)
33. Berberan-Santos M N, Bodunov E N, Pogliani L *J. Math. Chem.* **43** 1437 (2008)
34. NIST Chemistry WebBook, http://webbook.nist.gov/chemistry/
35. Simeoni G G et al. *Nature Phys.* **6** 503 (2010)
36. Batschinski A *Ann. Physik* **324** 307 (1906)
37. Ben-Amotz D, Herschbach D R *Israel J. Chem.* **30** 59 (1990)
38. Xu J, Herschbach D R *J. Phys. Chem.* **96** 2307 (1992)
39. Apfelbaum E M, Vorob'ev V S *J. Chem. Phys.* **130** 214111 (2009)
40. Brazhkin V V et al. *Phys. Rev. E* **85** 031203 (2012)
41. Brazhkin V V et al. *Pis'ma Zh. Eksp. Teor. Fiz.* **95** 179 (2012) [*JETP Lett.* **95** 164 (2012)]
42. Maxwell J C *Phil. Trans. R. Soc. Lond.* **157** 49 (1867)
43. Pontecorvo E *Phys. Rev. E* **71** 011501 (2005)
44. Pilgrim W-C, Morcel Chr *J. Phys. Condens. Matter* **18** R585 (2006)
45. Kob W, Andersen H C *Phys. Rev. Lett.* **73** 1376 (1994)
46. Schrøder Th B et al. *J. Chem. Phys.* **112** 9834 (2000)
47. De Lorenzi-Venneri G, Chisolm E D, Wallace D C *Phys. Rev. E* **78** 041205 (2008)
48. Bencivenga F et al. *Europhys. Lett.* **75** 70 (2006)
49. Balucani U, Zoppi M *Dynamics of the Liquid State* (Oxford: Clarendon Press, 1994)
50. Bryk T et al. *J. Chem. Phys.* **133** 024502 (2010)
51. Bencivenga F et al. *Phys. Rev. Lett.* **98** 085501 (2007)
52. Bencivenga F et al. *J. Chem. Phys.* **130** 064501 (2009)
53. Reid R C, Sherwood Th K *The Properties of Gases and Liquids* 2nd ed. (New York: McGraw-Hill, 1966)
54. Zwanzig R, Mountain R D *J. Chem. Phys.* **43** 4464 (1965)
55. Kor S K, Tandon U S, Singh B K *Phys. Lett. A* **38** 187 (1972)
56. Lurie J B *J. Low Temp. Phys.* **10** 751 (1973)
57. Stishov S M *Pis'ma Zh. Eksp. Teor. Fiz.* **57** 189 (1993) [*JETP Lett.* **57** 196 (1993)]
58. Trachenko K *Phys. Rev. B* **78** 104201 (2008)
59. Malescio G *J. Phys. Condens. Matter* **19** 073101 (2007)
60. Hagen M H J et al. *Nature* **365** 425 (1993)
61. Gast A P, Russel W B *Phys. Today* **51** (12) 24 (1998)
62. Stishov S M *Usp. Fiz. Nauk* **114** 3 (1974) [*Sov. Phys. Usp.* **18** 625 (1975)]
63. Klein O *Medd. Vetenskapsakad. Nobelinst.* **5** (6) (1919)
64. Landau L D, Lifshitz E M *Statisticheskaya Fizika* (Statistical Physics) Ch. 1 (Moscow: Fizmatlit, 1995) [Translated into English: Vol. 1 (Oxford: Pergamon Press, 1980)]
65. Hoover W G, Gray S G, Johnson K W *J. Chem. Phys.* **55** 1128 (1971)
66. Zhakhovskii V V *Zh. Eksp. Teor. Fiz.* **105** 1615 (1994) [*JETP* **78** 871 (1994)]
67. Lagar'kov A N, Sergeev V M *Usp. Fiz. Nauk* **125** 409 (1978) [*Sov. Phys. Usp.* **21** 566 (1978)]
68. van Hecke M *J. Phys. Condens. Matter* **22** 033101 (2010)
69. Biroli G *Séminaire Poincaré* **13** 37 (2009)
70. Tamm I E *Usp. Fiz. Nauk* **76** 397 (1962) [*Sov. Phys. Usp.* **5** 173 (1962)]
71. Heyes D M, Brańka A C *Mol. Phys.* **107** 309 (2009)
72. Meier K "Computer simulation and interpretation of the transport coefficients of the Lennard-Jones model fluid", Dissertation ... for Degree of Doktor-Ingenieur (Hamburg: Univ. of the Federal Armed Forces Hamburg, 2002)
73. Agrawal R, Kofke D A *Mol. Phys.* **85** 43 (1995)